Virology | Full-Length Text

Identification of host essential factors for recombinant AAV transduction of the polarized human airway epithelium

Siyuan Hao,[1] Xiujuan Zhang,[1] Kang Ning,[1] Zehua Feng,[2] Soo Yeun Park,[2] Cagla Aksu Kuz,[1] Shane McFarlin,[1] Donovan Richart,[1] Fang Cheng,[1] Elizabeth Yan Zhang,[3] Aaron Zhang-Chen,[3] Ziying Yan,[2] Jianming Qiu[1]

AUTHOR AFFILIATIONS See affiliation list on p. 22.

ABSTRACT Recombinant (r)AAV2.5T was selected from the directed evolution of an adeno-associated virus (AAV) capsid library in the human airway epithelium (HAE). The capsid gene of rAAV2.5T is a chimera of the N-terminal unique coding sequence of AAV2 VP1 unique (VP1u) and the VP2- and VP3-coding sequences of AAV5 with a single amino acid mutation of A581T. We conducted two rounds of genome-wide CRISPR guide (g)RNA library screening for host factors limiting rAAV2.5T transduction in HeLa S3 cells. The screening identified several genes that are critical for rAAV2.5T, including the previously reported genes *KIAA0319L*, *TM9SF2*, *VPS51*, and *VPS54*, as well as a novel gene *WDR63*. We verified the role of KIAA0319L and WDR63 in rAAV2.5T transduction of polarized HAE by utilizing CRISPR gene knockouts. Although KIAA0319L, a proteinaceous receptor for multiple AAV serotypes, played an essential role in rAAV2.5T transduction of polarized HAE either from the apical or basolateral side, our findings demonstrated that the internalization of rAAV2.5T was independent of KIAA0319L. Importantly, we confirmed that WDR63 is an important player in rAAV2.5T transduction of HAE while not being involved in vector internalization and nuclear entry. Furthermore, we identified that the basal stem cells of HAE can be significantly transduced by rAAV2.5T.

IMPORTANCE The essential steps of successful gene delivery by recombinant adeno-associated viruses (rAAVs) include vector internalization, intracellular trafficking, nuclear import, uncoating, double-stranded (ds)DNA conversion, and transgene expression. rAAV2.5T has a chimeric capsid of AAV2 VP1u and AAV5 VP2 and VP3 with the mutation A581T. Our investigation revealed that KIAA0319L, the multiple AAV serotype receptor, is not essential for vector internalization but remains critical for efficient vector transduction to human airway epithelia. Additionally, we identified that a novel gene *WDR63*, whose cellular function is not well understood, plays an important role in vector transduction of human airway epithelia but not vector internalization and nuclear entry. Our study also discovered the substantial transduction potential of rAAV2.5T in basal stem cells of human airway epithelia, underscoring its utility in gene editing of human airways. Thus, the knowledge derived from this study holds promise for the advancement of gene therapy in the treatment of pulmonary genetic diseases.

KEYWORDS rAAV2.5T, KIAA0319L, WDR63, transduction, human airway epithelium

Adeno-associated viruses (AAVs) are members of the genus *Dependoparvovirus* of the *Parvoviridae* family (1). AAV is non-enveloped and has a single-stranded (ss)DNA genome of 4.7 kb. It is nonpathogenic to humans and replication-deficient *per se*. It requires a helper virus, e.g., adenovirus (Ad), to replicate. Recombinant (r)AAVs are considered a safe transduction vector for *in vivo* gene transfer in the application of human gene therapy (2, 3). Since the late 1990s, rAAVs have been used in a number of clinical trials to treat a wide variety of monogenetic disorders across target organs,

including the lung, eye, liver, and skeletal muscle (4–8). So far, the US Food and Drug Administration (FDA) has approved four rAAV-based gene therapy medicines, LUXTURNA, ZOLGENSMA, HEMGENIX, and ELEVIDYS, for the treatment of Leber congenital amaurosis, spinal muscular atrophy, hemophilia B, and Duchenne muscular dystrophy, respectively.

One major hurdle in rAAV-based gene therapy is the requirement of a high vector dose. Although rAAVs have been extensively used in biomedical research and gene therapy, there is still limited understanding of how they enter cells and deliver their cargo to the nucleus. Additionally, the essential host factors that facilitate transgene expression vary depending on the specific AAV serotype and the type of cells being targeted (9). The cell and tissue tropism of an AAV is determined by its capsid structure, which is composed of viral proteins VP1, VP2, and VP3 at a molar ratio of ~1:1:10 (10), and by its interaction with the specific surface receptors and host factors present on or within the target cells. In general, the cell attachment of most AAV serotypes is mediated by capsid-specific glycan moieties on the cell surface that have been studied extensively (11). After attachment, AAVs are internalized into the target cell through receptor-mediated endocytosis. Previously, a genetic screening identified a highly conserved AAV entry factor, KIAA0319L, as a cellular receptor for certain naturally occurring AAVs (AAV1, 3, 5, 6, 8, and 9) (12). However, it is important to note that AAV4-like AAVs (AAV4, AAV11, and AAV12) do not utilize KIAA0319L for vector transduction (13). KIAA0319L is classified as a type I transmembrane protein. The purified recombinant KIAA0319L or an anti-KIAA0319L antibody effectively inhibits transduction of rAAV1-3, 5, 6, 8, and 9, and the knockout of *KIAA0319L* in *in vitro* cultured cell lines or mice resulted in resistance to rAAV transduction (12). Although KIAA0319L was characterized as an N- and O-glycosylated cell membrane protein, glycosylation does not contribute to AAV binding and transduction (14). It appears transiently on the cell surface but localizes primarily to the perinuclear trans-Golgi network (TGN). While the native role of KIAA0319L is presumed to involve acting as a recycling receptor for an unidentified ligand, it has been identified as a proteinaceous receptor for certain AAV serotypes. AAV has evolved to exploit the retrograde trafficking of KIAA0319L. However, the precise mechanism by which KIAA0319L facilitates rAAV transduction remains elusive, specifically its involvement in AAV cell surface binding, AAV internalization, intracellular trafficking, potential interacting partners, and its recycling route from the cell surface to the TGN.

Even though it remains unclear how AAV capsids differentially interact with host factors, AAV capsids can be engineered to modify their cell/tissue tropism by introducing specific mutations that enhance or alter their interactions with receptors and/or cellular factors relevant to the desired target cells or tissues. AAV2.5T is an airway tropic AAV variant identified from the directed evolution of an AAV capsid library in polarized human airway epithelia. The VP1 of AAV2.5T is a chimeric protein composed of the AAV2 VP1u region [amino acids (aa) 1–118] with the remaining aa 119–725 from AAV5 VP1, along with a key point mutation (A581T), and the VP2 and VP3 of AAV5 bearing the same mutation (15). The rAAV2.5T vector demonstrated a greater than 10-fold improvement over AAV2 and AAV5 in the transduction of human airway epithelia (15). It efficiently transduces cystic fibrosis (CF) human airway epithelia from the apical side. rAAV2.5T successfully delivered the expression of the CF transmembrane conductance regulator minigene (CFTRΔR) with a 156-bp deletion in the regulatory (R) domain (16) to correct the deficient transepithelial transport of chloride anions in polarized human airway epithelia derived from CF lung donors (15, 17).

Similar to its parent AAV5, AAV2.5T uses cell surface α2,3 N-linked sialic acid (SA) as the primary attachment receptor (18). The SA-binding sites of AAV5 were mapped to M569, A570, T571, G583, T584, Y585, N586, and L587, and the binding pocket has a contact distance of 2.4–3.6 Å to interact with SA (19). While the A581T mutation is close to the SA binding site, its impact on SA binding is minimal due to the fact that the binding affinities of AAV5 and AAV2.5T to α2,3 N-linked SA remain similar (18), suggesting that both use the same mechanism to bind SA.

Understanding the important host factors that facilitate rAAV2.5T transduction in human airway epithelia is crucial to fully exploit the potential of this novel vector in CF gene therapy. In this study, we first undertook a genome-wide CRISPR screening in HeLa S3 cells. We found that guide (g)RNAs targeting the gene *KIAA0319L* had the highest enrichment score from the analysis of the screening. Importantly, our study also identified that the gene *WDR63* is important for AAV2.5T transduction of human airway epithelia. Interestingly, our vector internalization assays demonstrated that neither KIAA0319L nor WDR63 plays a role in the internalization of rAAV2.5T into the cells of human airway epithelia. Thus, our findings indicate that KIAA0319L may function differently in different types of cells and tissues for rAAV transduction.

RESULTS

Genome-wide CRISPR screening identifies novel essential factors of rAAV2.5T transduction

The capsid of AAV2.5T differs from that of AAV5 by only a single amino acid (A581T) in VP2 and VP3, while the N-terminus of VP1, which is replaced by the VP1u of AAV2, remains concealed inside the capsid. While AAV5 interacts with KIAA0319L to promote transduction in HeLa cells (14), it has been reported that rAAV2.5T transduction in HeLa cells or apical transduction of polarized human airway epithelia is independent of KIAA0319L (20), suggesting that rAAV2.5T and rAAV5 exploit different mechanisms for transduction. To explore the specific receptors and co-receptors involved in rAAV2.5T entry into human airway epithelia, we utilized a genome-wide CRISPR pooled gRNA library for high-throughput screening to identify the significant host factors that restricted rAAV2.5T transduction in HeLa S3 cells. To facilitate the screening, suspension HeLa S3 cells were transduced with a lentiviral vector to incorporate the expression of *Streptococcus pyogenes* (sp)Cas-9. These spCas9-expressing HeLa S3 cells were transduced with the lentiviral-based pooled gRNA library (Brunello) for human gene knockouts at a multiplicity of infection (MOI) of 0.25 transduction units/cell to ensure that each cell was transduced by no more than one gRNA-expressing lentivirus. Following the selection of cells with puromycin at 2 µg/mL, the spCas9 and single (s)gRNA-expressing HeLa S3 cells were extracted for genomic DNA (gDNA), designated as gDNA^{Ctrl}. For the screening, we transduced the spCas9 and sgRNA library-expressing HeLa S3 cells with mCherry-expressing rAAV2.5T (rAAV2.5T.F5tg83luc-CMVmCherry) at an MOI of 20,000 DNase-resistant particles (DRPs)/cell, by which a transduction efficiency of 96.4% (mCherry positive) was achieved. Using flow cytometry, we sorted ~1 million mCherry-negative cells and amplified them for the second round of transduction of rAAV2.5T at the same MOI. Again, ~1 million mCherry-negative cells were sorted, expanded, and subjected to extraction of gDNA that was designated as gDNA^{Screen} (Fig. 1A). Both gDNA^{Ctrl} and gDNA^{Screen} were subjected to next-generation sequencing (NGS) to probe the sgRNAs enriched in the transduction-restricted cells. Analysis using the bioinformatics software MAGeCK highlighted the sgRNAs that were significantly enriched in the second round of sorted mCherry-negative cells compared to unselected control cells (Table S1; Fig. S1). The genes that have an enrichment score of >3.25 are shown in Fig. 1B. Most notably, *KIAA0319L*, which was previously reported as a multi-serotype AAV receptor (12), was the top selected gene (Fig. 1B). Gene ontology (GO) classification showed many potential rAAV2.5T host essential factors identified in our screening, including TM9SF2, VPS51, and VPS54, which were previously identified as the host essential factors for rAAV transduction (11).

HeLa cell screening identifies *KIAA0319L*, *TM9SF2*, and *WDR63* as important host genes

We selected the top 27 candidates with an enrichment score of >3.25 (Fig. 1B) and available antibodies to verify their roles in rAAV2.5T transduction in HeLa cells. We first used shRNA-expressing lentiviruses to selectively silence the expression of these
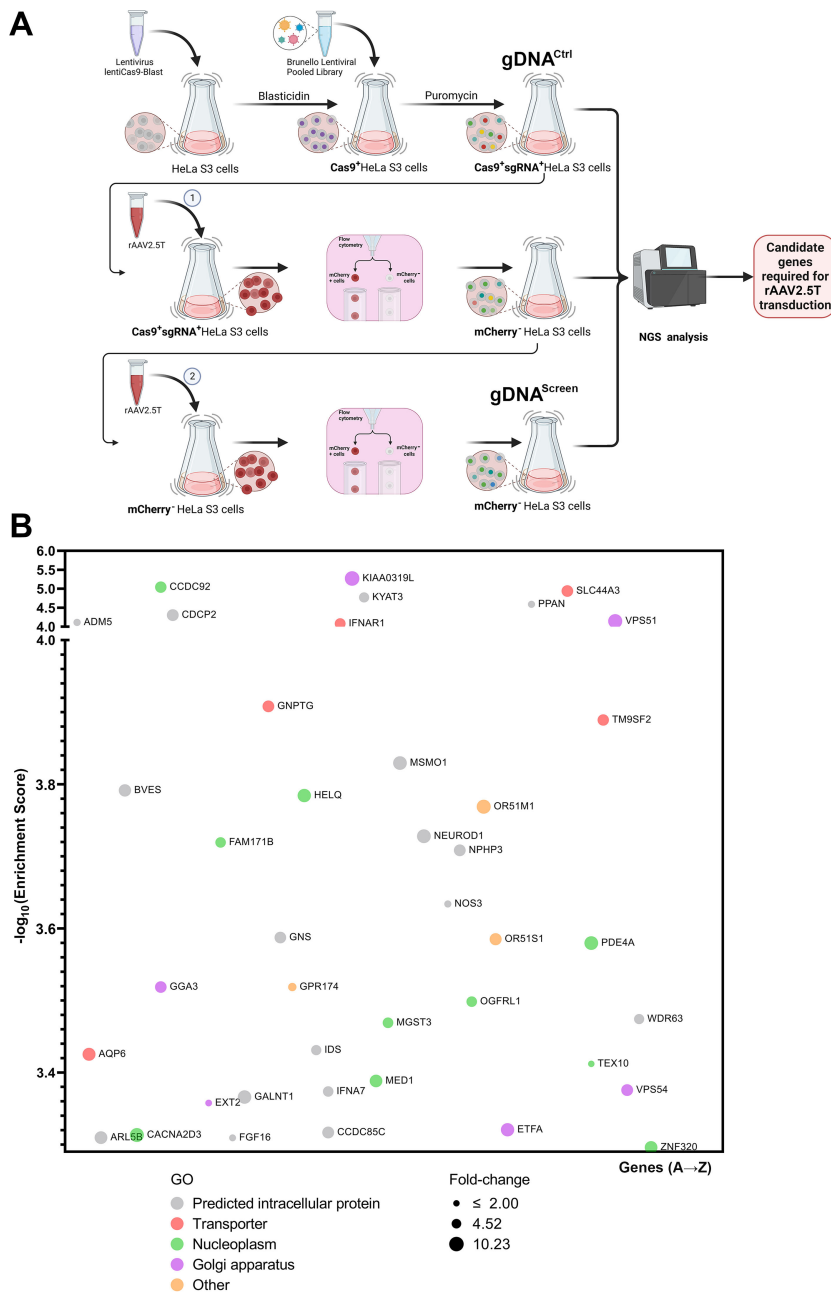
FIG 1 Genome-wide guide RNA (gRNA) library screening of essential factors of rAAV2.5T transduction in HeLa S3 cells. (A) A diagram of the genome-wide gRNA library screening. HeLa S3 suspension cells were transduced with a spCas9-expressing lentivirus. Blasticidin-resistant spCas9-expressing cells were transduced with the Brunello lentiCRISPR gRNA lentiviral library. The library-selected HeLa S3 cells were expanded to ~200 million, of which ~100 million were extracted for genomic DNA (gDNA) as the non-selected control gDNA (gDNA^{Ctrl}), and another 100 million were transduced with mCherry-expressing rAAV2.5T. At 3 days post-transduction, ~1 million mCherry-negative cells were sorted and expanded. Approximately 100 million cells were transduced with rAAV2.5T, followed by sorting of the top 1% mCherry-negative cells. The sorted mCherry-negative cells were expanded to ~100 million for extraction of gDNA^{Screen}. The gDNA samples were subjected to NGS analysis and bioinformatics analysis. Created with BioRender. (B) Hits of host genes from the second round of screening of mCherry-negative cells. This panel shows the entry screening hits from the second-round selection of mCherry-negative cells transduced with rAAV2.5T. The x-axis shows genes within the target of the Brunello library that are

(Continued on next page)

FIG 1 (Continued)

grouped by gene ontology analysis. Each circle represents a gene with the size corresponding to the fold change of sgRNA reads by comparison of gDNA^{Screen} to gDNA^{Ctrl}. The y-axis shows the enrichment score ($-\log_{10}$) of each gene based on MAGeCK analysis of the sgRNA reads in gDNA^{Screen} vs gDNA^{Ctrl}. Only genes that have an enrichment score of >3.25 are shown. The bubble colors indicate different gene ontology classifications as shown.

candidate genes, respectively, in HeLa cells. The 27 candidate genes were silenced to different extents, as shown by Western blotting (Fig. S2). The dual-reporter rAAV2.5 vector, rAAV2.5T.F5tg83luc-CMVmCherry, was used to transduce these individually gene-silenced HeLa cells at an MOI of 20,000. At 3 days post-infection, the transduction efficiencies were assessed for mCherry expression and luciferase activity using flow cytometry and firefly luciferase activity assays, respectively. After normalization of mCherry expression with scramble (non-target) shRNA control cells, the data showed that silencing of *KIAA0319L*, *KYAT3*, *TM9SF2*, *NPHP3*, *WDR63*, and *ZNF320* decreased mCherry expression by >50% (Fig. 2A, columns in red). Silencing of *CCDC92*, *CDCP2*, *MSMO1*, *OR51M1*, *PDE4A*, and *GPR174* decreased mCherry expression by >25% but <50% (Fig. 2A, columns in green). Similarly, we found that silencing of *KIAA0319L*, *TM9SF2*, *WDR63*, and *ZNF320* decreased luciferase expression by >50% (Fig. 2B, columns in red) and that silencing of *KYAT3*, *OR51M1*, *NPHP3*, and *PDE4A* decreased luciferase expression by >25% but <50% (Fig. 2B, columns in green).

We plotted relative expression values ($-\log_2$) of both luciferase and mCherry expressions (Fig. 2C). The genes whose silencing decreased both expressions are shown in quadrant I, with *KIAA0319L* being the highest and *TM9SF2* being the second-highest hit. Both have been shown to be essential entry factors of transduction in whole-genome gRNA library screens using rAAV2 (12, 21). We finally narrowed the candidate essential factor genes down to 11, i.e., *KIAA0319L*, *TM9SF2*, *ZNF320*, *WDR63*, *KYAT3*, *NPHP3*, *PDE4A*, *OR51M1*, *CCDC92*, *MSMO1*, and *GPR174*. Then, we looked back to our NGS data for these 11 genes (Fig. S3) and found that most of the genes showed an average of >2,000-fold enrichment in sgRNA reads compared to the unselected control, indicating that these candidates are highly likely to play a role in rAAV2.5T transduction.

Next, we examined the role of these 11 candidate genes in rAAV2.5T transduction in gene knockout HeLa cells. To this end, HeLa cells were transduced with individual sgRNA-expressing lentiviral vectors and underwent single-cell expansion. Western blotting demonstrated a drastic decrease in the expression of all the selected candidate genes (Fig. 3A). Then, each line of the gene knockout cells was infected with rAAV2.5T. The results showed that the *KIAA0319L* knockout decreased luciferase expression by >90%, and the *TM9SF2* and *WDR63* knockouts decreased luciferase expression by >60% (Fig. 3B). Notably, the *WDR63* knockout decreased luciferase expression to the same level as the *TM9SF2* knockout. In addition, the *PDE4A* and *GPR174* knockouts showed ~50% decreases in luciferase expression. However, the *ZNF320*, *KYAT3*, and *CCDC92* gene knockouts did not show any significant decrease in luciferase expression when compared to the non-target control (Fig. 3B).

Collectively, we confirmed that *KIAA0319L*, *TM9SF2*, and *WDR63* are the top three host genes important for transduction and that *PDE4A* and *GPR174* also play a significant role in rAAV2.5T transduction in HeLa cells.

KIAA0319L and *WDR63* knockouts significantly decrease AAV2.5T transduction in HAE-ALI cultures

Since rAAV2.5T has a high tropism to human airway epithelia (15, 18), we investigated the function of *KIAA0319L* and *WDR63* in rAAV2.5T transduction of the polarized human airway epithelium cultured at an air-liquid interface (HAE-ALI). To this end, we used gRNA-expressing lentiviruses to knock out *KIAA0319L* and *WDR63*, respectively, in an immortalized human airway epithelial cell line, CuFi-8. CuFi-8 cells maintain a phenotype
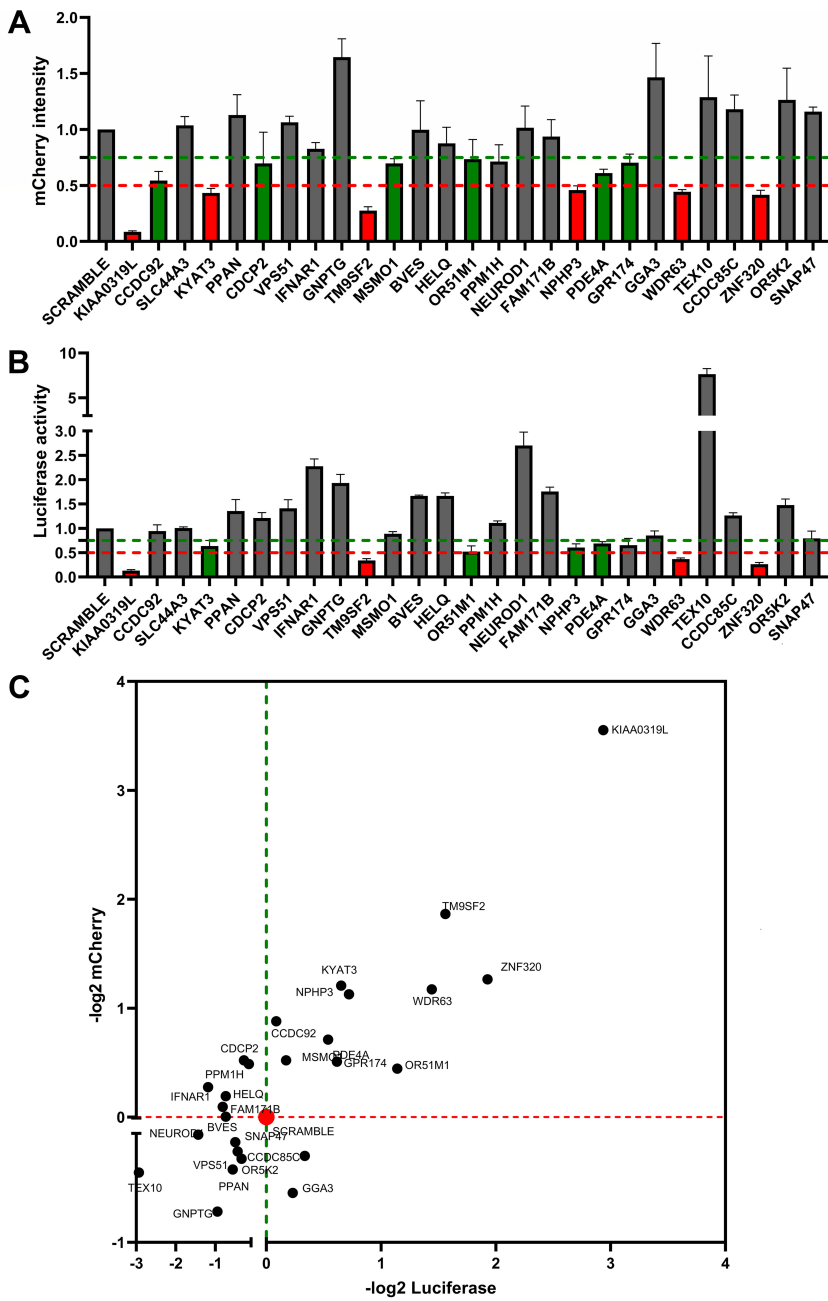
FIG 2 rAAV2.5T transduction in the 28 top-ranking gene-silenced HeLa cells. (A and B) Relative expression of luciferase and mCherry in gene-silenced cells. HeLa cells seeded in 24-well plates were transduced with a shRNA-expressing lentiviral vector. After selection in puromycin, the cells were transduced with rAAV2.5T at an MOI of 20,000 DRPs/cell. At 3 days post-transduction, mCherry expression was imaged under a fluorescence imager (A), and the luciferase activity was measured using a firefly luciferase detection reagent (B). All data had three repeats and were normalized to the non-target (NT) control. The green and red dashed lines indicate 75% and 50% of the NT control, respectively. Data shown are means with a standard deviation (SD) from three replicates. (C) Ranks of the candidates in quadrant I. The x-axis shows $-\log_2$ luciferase intensity, and the y-axis shows $-\log_2$ mCherry intensity. All the cells silenced with gene names shown in quadrant I had decreases in both luciferase and mCherry expressions.

of airway basal cells in proliferating cultures and can undergo differentiation into pseudostratified HAE when cultured at an ALI (22) (Fig. 4A). After confirmation of the gene knockout in proliferating CuFi-8 cells by Western blotting and genomic DNA
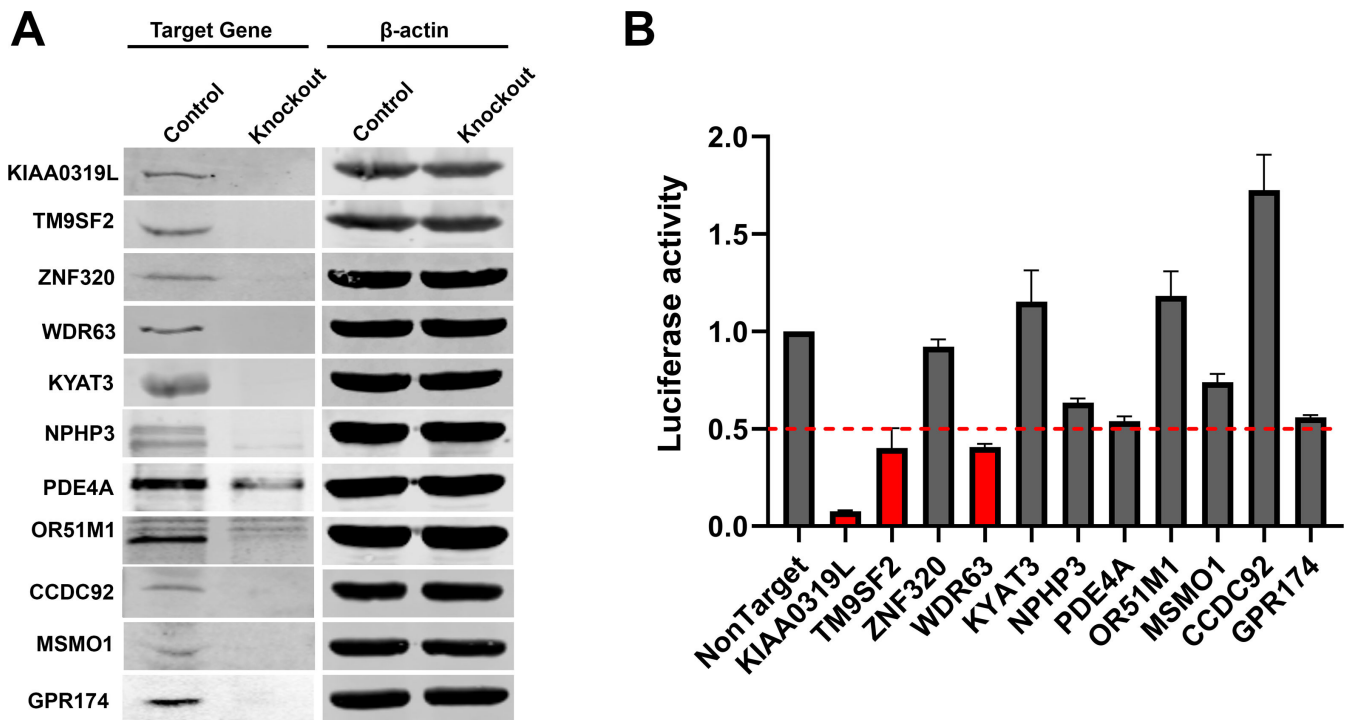
FIG 3 rAAV2.5 transduction of individual gene knockout HeLa cells. Eleven candidate genes (*KIAA0319L*, *TM9SF2*, *ZNF320*, *KYAT3*, *NPHP3*, *WDR63*, *PDE4A*, *OR51M1*, *GPR174*, *CCDC92*, and *MSMO1*) were selected based on the shRNA knockdown screening. A gRNA-expressing lentiviral vector was applied to HeLa cells, and single-cell cloning was carried out to generate a knockout cell line. (A) Western blotting. Western blots show the knockout efficiency at 3 days post-transduction. β-Actin was used as a loading control. (B) Luciferase activities in gene knockout HeLa cells. Gene knockout cells were transduced with rAAV2.5T at an MOI of 20,000 DRPs/cell. At 3 days post-transduction, the luciferase activities were measured. The red dashed line indicates 50% of the luciferase activity in non-target control HeLa cells. Data shown are means with an SD from three replicates.

sequencing (Fig. 4B), we seeded the gene knockout CuFi-8 cells on collagen-coated transwells to differentiate them into HAE-ALI cultures. The maturation of epithelial differentiation is indicated by a value >1,000 $\Omega\cdot cm^2$ of transepithelial electrical resistance (TEER). After 3 weeks of differentiation at ALI, the TEER of the HAE-ALI$^{\Delta KIAA0319L}$ and HAE-ALI$^{\Delta WDR63}$ cultures, as well as the non-target (NT) control cultures, was measured. The TEER readings of these cultures approached ~2,000 $\Omega\cdot cm^2$, indicating that the HAE-ALI cultures were fully differentiated (Fig. 4C). We also examined epithelial tight junction formation and cilial development by immunofluorescence staining for the tight junction protein ZO-1 and the cilial development marker β-tubulin IV. As shown in Fig. 4D, both the *KIAA0319L* and *WDR63* knockouts did not obviously change the structure of ZO-1 and cilia. Thus, we successfully developed HAE-ALI cultures with the *KIAA0319L* or *WDR63* gene knockouts with retained tight junction and cilia structures, as well as normal epithelial barrier function.

Next, the HAE-ALI$^{\Delta KIAA0319L}$ and HAE-ALI$^{\Delta WDR63}$ cultures were infected with rAAV2.5T at an MOI of 20,000 from the apical side (Fig. 5A) or the basolateral side (Fig. 5B). Infection of HAE-ALI^{NT} was included as the NT control. At 5 days post-transduction, the rAAV2.5T transduction efficiency was assessed by mCherry fluorescence and luciferase activity. HAE-ALI$^{\Delta KIAA0319L}$ and HAE-ALI$^{\Delta WDR63}$ showed a significant decrease in both mCherry and luciferase expressions from the transduction at either the apical or basolateral side compared to the NT control (Fig. 5A through D). The luciferase quantification demonstrated that the knockouts of KIAA0319L and WDR63 decreased apical transduction by >70% and 71%, as well as basal transduction by >88% and 64%, respectively, compared to the NT control (Fig. 5C and D). For all three types of HAE-ALI cultures, transduction at the apical side was higher than that at the basolateral side.
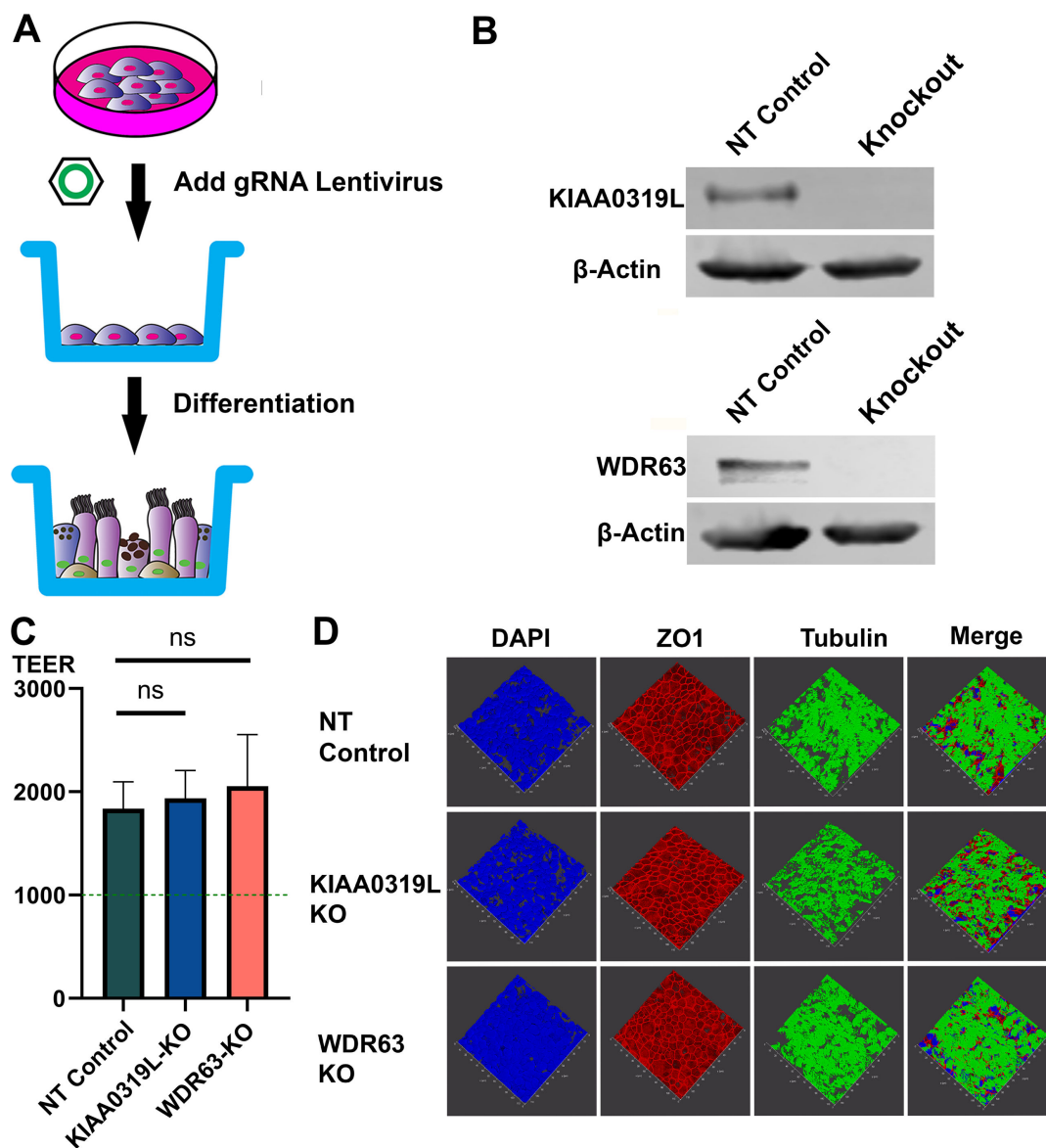
FIG 4 Generation of gene knockouts in HAE-ALI cultures (A) Knockouts of *KIAA0319L* and *WDR63* in HAE-ALI cultures. A schematic diagram shows the generation of gene knockouts of CuFi-8-derived HAE-ALI cultures. CuFi-8 cells were cultured in collagen-coated 100-mm dishes until confluent, and then gRNA-expressing lentiviruses were added to the dishes. Under the selection of puromycin, the CuFi-8 cells were single-clone expanded for the production of a gene knockout cell line. Expanded gene knockout cells were transferred onto the transwell for polarization at ALI. (B) Gene knockdown efficiency. Western blotting and genomic DNA sequencing validated the knockouts of *KIAA0319L* and *WDR63* in HAE-ALI cultures. Cells harvested from the transwells were extracted for proteins and DNA, respectively. Western blotting detected both the non-target control and knockout groups, KIAA0319L and WDR63, respectively. β-Actin was detected as a loading control. The genomic DNA was amplified for sequencing the mutations at the gRNA targeting sequences of the *KIAA0319L* and *WDR63* genes, respectively. The gene sequences show the original gene sequence, the non-target gene sequence, and the gene knockout sequence. (C) TEER measurement. After 1 month of differentiation at ALI, HAE-ALI cultures, non-target NT (NT) control, KIAA0319L-KO, and WDR63-KO, were detected for TEER values. Data shown are means with an SD of three replicates. (D) Three-dimensional confocal imaging of ZO-1 and β-tubulin expression in gene knockout HAE-ALI. NT, KIAA0319L-KO, and WDR63-KO HAE-ALI cultures were fixed and co-stained with anti-β-tubulin IV (green) and anti-ZO-1 (red) antibodies. Nuclei were stained with DAPI (blue). A set of confocal images was taken at a magnification of ×40 (Leica SP8 STED) from the stained piece of the epithelium from the objective (z-axis) and reconstituted as a three-dimensional image as shown in each channel of fluorescence.

As KIAA0319L was reported to function as a multi-serotype AAV receptor (12–14), we carried out a vector internalization assay to examine the role of KIAA0319L and WDR63 in vector endocytosis. The internalization assay showed that both HAE-ALI$^{\Delta KIAA0319L}$ and HAE-ALI$^{\Delta WDR63}$ did not have a significant decrease in the levels of internalized vectors

FIG 5 Knockouts of KIAA0319L and WDR63 cause a significant decrease in the transduction efficiency of rAAV2.5T in HAE-ALI cultures but not vector internalization. HAE-ALI cultures were transduced with rAAV2.5T at an MOI of 20,000 DRPs/cell from the apical (left panels A, C, and E) and basolateral chambers (right panels B, D, and F), respectively. At 16 hours post-transduction, both the apical and basolateral chambers were refreshed with culture media. (A and B) mCherry expression. Images were taken under a fluorescence imager at 5 days post-transduction. (C and D) Luciferase activity assay. Luciferase activity was measured at 5 days post-transduction. Data shown are means with an SD from three replicates. (E and F) Vector internalization assay. HAE-ALI cultures were incubated with rAAV2.5T at an MOI of 20,000 DRPs/cell from the apical and basolateral chambers, respectively, for 2 hours at 37°C. Then, the viruses were removed, and both chambers were treated with Accutase three times. Viral DNA was extracted using the pathogen viral DNA collection kit (Zymo) and quantified via quantitative polymerase chain reaction (qPCR) using an mCherry gene-targeting probe to detect the entered viral genomes. The boundary of the box closest to zero indicates the 25th percentile, a black line within the box marks the median, and the boundary of the box farthest from zero indicates the 75th percentile. Whiskers above and below the box indicate the 10th and 90th percentiles.

compared to the HAE-ALI^{NT} control from transduction either at the apical or basolateral side (Fig. 5E and F). In contrast, internalization assays in HeLa cells showed that KIAA0319L-KO HeLa cells showed a threefold decrease in vector internalization compared with the control HeLa cells (Fig. S4). Therefore, our virus internalization argues against the role of KIAA0319L in rAAV2.5T entry into human airway epithelia.

Doxorubicin (Dox), an FDA-approved drug for cancer therapy, has been used as a potent agent to augment AAV-mediated transgene expression, especially in airway epithelia, functioning as a proteasome inhibitor to prevent the degradation of ubiquitinated AAV in the cytoplasm and facilitate vector nuclear import (23). We used rAAV2.5T to transduce HAE-ALI cultures in the presence of Dox at 2 µM during a 16-hour infection period. Dox treatment significantly increased mCherry expression from rAAV2.5T apical and basal transduction in HAE-ALI cultures at 5 days post-transduction (Fig. 6A and B) compared to the no-Dox treatment control (Fig. 5A and B). From the luciferase activity, Dox treatment increased the rAAV2.5T transduction by 59- and 37-fold from the transduction of the apical and basolateral sides, respectively (Fig. 6C and D). Luciferase activity was decreased in HAE-ALI$^{\Delta KIAA0319L}$ by 93% and 95%, respectively, from the transduction of apical and basolateral sides, and a 77% and 81% decrease in HAE-ALI$^{\Delta WDR63}$ (Fig. 6C and D). Importantly, in Dox-treated HAE-ALI, we also found that both HAE-ALI$^{\Delta KIAA0319L}$ and HAE-ALI$^{\Delta WDR63}$ did not show any significant decrease in vector internalization during either apical or basolateral transduction at 37°C for 2 hours (Fig. 6E and F).

Taking all these results together, although the *KIAA0319L* and *WDR63* knockouts drastically reduced rAAV2.5T transduction in HAE-ALI cultures, the lack of KIAA0319L and WDR63 expressions did not affect vector internalization into the cells during either apical or basolateral transduction. Notably, the treatment with Dox did not influence the entry of rAAV2.5T in HAE-ALI from either the apical or basal side, consistent with previous observations in the transduction of other AAV serotypes in HAE-ALI, with less efficiencies (23).

Cellular localization of KIAA0319L and WDR63 in the major types of airway epithelial cells of HAE-ALI cultures

Human airways are lined by a variety of cell types (24). The surface layer is primarily populated with ciliated cells as well as goblet and club secretory cells, the intermediate cells are club cells that can be differentiated into ciliated or secretory cells, and the basal stem cells are secured to the basement membrane. Thus, we investigated the transduction efficiency of rAAV2.5T in the four major epithelial cell types: ciliated, basal, club, and goblet cells. Using flow cytometry of the cells dissociated from the inserts, we first determined that the CuFi-8-derived HAE-ALI cultures were composed of ciliated, basal, club, and goblet cells at percentages of approximately 50%, 24%, 22%, and 4%, respectively (Fig. 7A). Next, we analyzed rAAV2.5T-transduced HAE-ALI cultures and found that there were ~35.4% mCherry-positive cells in the transduced cultures. Then, mCherry-positive cells were sorted and analyzed by flow cytometry for the percentages of the four cell types using cell type-specific antibodies. We determined that 45%, 19.5%, 34%, and 1.5% of the ciliated, basal, club, and goblet cells, respectively, were present in the rAAV2.5T-transduced HAE-ALI cultures (mCherry-positive cell population) (Fig. 7B). Immunofluorescence analyses using antibodies against specific cell-type markers revealed that the four major types of airway epithelial cells in HAE-ALI were transduced by rAAV2.5T, albeit at various levels (Fig. 7C).

Knowing the localization of KIAA0319L and WDR63 in cells is critical to understand their functions during rAAV2.5T transduction of HAE-ALI. We carried out immunofluorescence staining to reveal the cellular localization of KIAA0319L and WDR63. The results showed that KIAA0319L localized on both the cell surface and in the cytoplasm of the four types of epithelial cells of HAE-ALI treated with Dox and apically transduced with rAAV2.5T (Fig. 8A), indicating that KIAA0319L is likely to participate in the intracellular
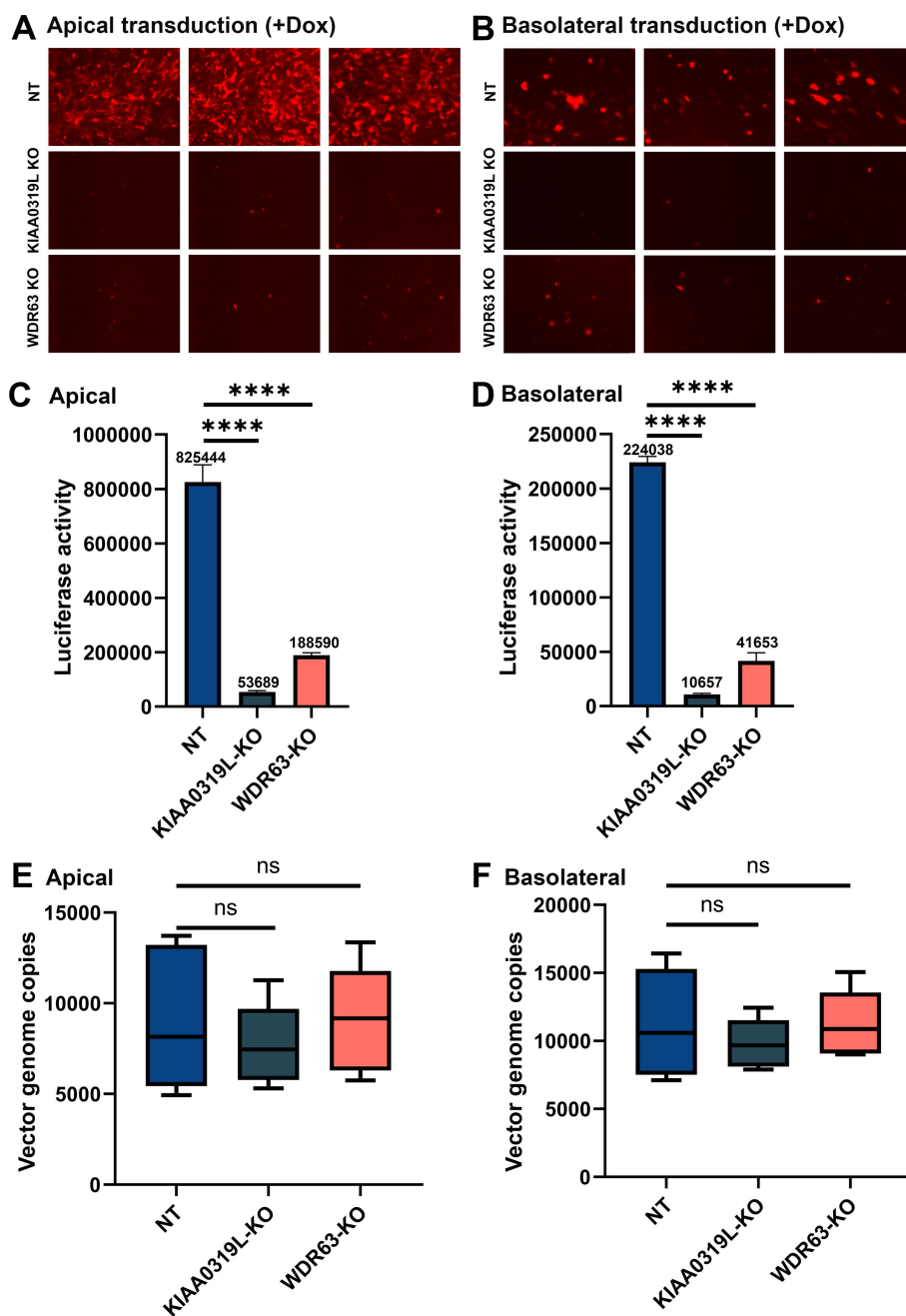
FIG 6 Knockouts of *KIAA0319L* and *WDR63* cause a significant decrease in the transduction efficiency of rAAV2.5T in Dox-treated HAE-ALI cultures but not vector internalization. HAE-ALI cultures were transduced with rAAV2.5T at an MOI of 20,000 DRPs/cell from the apical (left panels A, C, and E) and basolateral chambers (right panels B, D, and F), respectively. Dox was added to rAAV2.5T at 2.0 µM. At 16 hours post-transduction, both the apical and basolateral chambers were refreshed with culture media. (A and B) mCherry expression. Images were taken under a fluorescence imager at 5 days post-transduction. (C and D) Luciferase activity assay. Luciferase activity was measured at 5 days post-transduction. Data shown are means with an SD from three replicates. (E and F) Vector internalization assay. HAE-ALI cultures were transduced with rAAV2.5T from the apical and basolateral chambers, respectively, for 2 hours at 37°C. Then, the vectors were removed, and both chambers were treated with Accutase three times. Viral DNA was extracted and quantified via qPCR. The boundary of the box closest to zero indicates the 25th percentile, a black line within the box marks the median, and the boundary of the box farthest from zero indicates the 75th percentile. Whiskers above and below the box indicate the 10th and 90th percentiles.
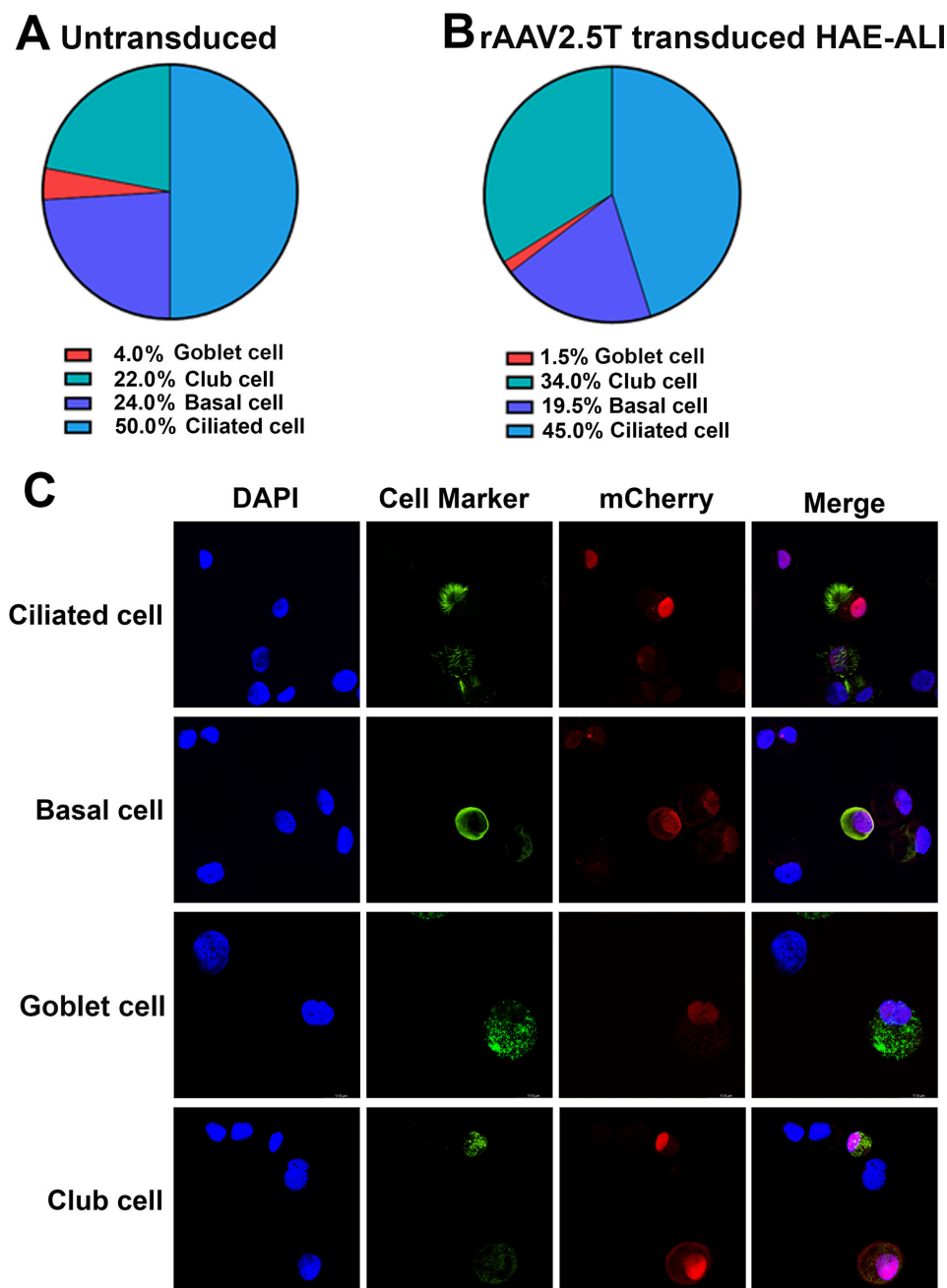
FIG 7 Analysis of rAAV2.5T-transduced cell types in HAE-ALI cultures. HAE-ALI cultures were transduced with rAAV2.5T at an MOI of 20,000 DRPs/cell from the apical chamber or mock transduced. Dox was added to rAAV2.5T at 2.0 µM. (A) Flow cytometry of airway cell types in HAE-ALI cultures. The cells of the mock-transduced HAE-ALI cultures were digested off the transwell membranes, fixed, and permeabilized, followed by immunostaining with the primary antibody against each cell marker and an Alexa 488-conjugated secondary antibody. The stained cells were subjected to flow cytometry, and the percentage of each cell type was calculated. (B) Flow cytometry of airway cells transduced with rAAV2.5T. At 7 days post-transduction, the cells of the rAAV2.5T-transduced HAE-ALI cultures were digested off the transwell membranes and sorted on a BD FACSAria III Cell Sorter. mCherry-positive cells were sorted by FACS, fixed, and permeabilized, followed by immunostaining with the primary antibody against each cell marker and an Alexa 488-conjugated secondary antibody. The stained cells were subjected to flow cytometry, and the percentage of each cell type was calculated. (C) Immunofluorescence assays. At 7 days post-transduction, the cells of rAAV2.5T-transduced HAE-ALI cultures were digested off the transwell membranes, cytospun to slides, fixed, and permeabilized, followed by immunostaining with an antibody against each cell marker. The stained cells were subjected to imaging under confocal microscopy at a magnification of ×100 (CSU-W1 SoRa, Nikon).

trafficking of rAAV2.5T (25). Strikingly, WDR63 localized in both the nucleus and the cytoplasm with a preference for the nucleus (Fig. 8B).

Lastly, we investigated rAAV2.5T capsid distribution in HAE-ALI cells using immunofluorescence assays. In ciliated cells, the nuclear entry of rAAV2.5T vectors was observed in non-target control and HAE-ALI$^{\Delta WDR63}$ cultures, but vector particles were scarcely found within the nuclei of cells in HAE-ALI$^{\Delta KIAA0319L}$ cultures (Fig. 9A). We also observed that no vector particles entered the nuclei of the club cells of the HAE-ALI$^{\Delta KIAA0319L}$, but more vector particles entered the nuclei of the cells of the non-target control and HAE-ALI$^{\Delta WDR63}$ cultures (Fig. 9B). We also fractionated the nucleus and cytosol of the three types of HAE-ALI cultures and quantified the vector genome in both fractions. We found that vector genomes in the nuclei of HAE-ALI$^{\Delta KIAA0319L}$ were significantly decreased from 63.5% to 40.3% but significantly increased in the nuclei of HAE-ALI$^{\Delta WDR63}$ from 63.5% to 70.5% compared with the NT control (Fig. 9C), suggesting that WDR63 may
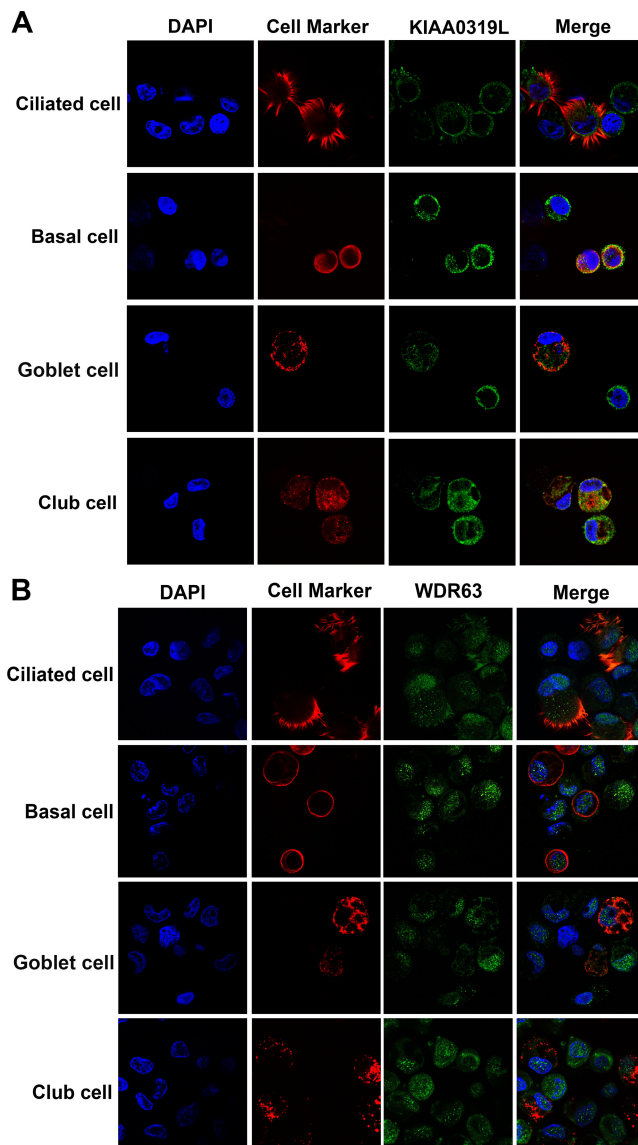

FIG 8 Localization of KIAA0319L and WDR63 in airway epithelial cells of HAE-ALI cultures. The cells of HAE-ALI cultures were digested off the transwell membranes with Accutase, fixed, and permeabilized, followed by co-immunostaining with an antibody against each cell marker and anti-KIAA0319L (A) or anti-WDR63 (B), followed by staining with a corresponding secondary antibody. The stained cells were subjected to imaging under confocal microscopy at a magnification of ×100 (CSU-W1 SoRa, Nikon).
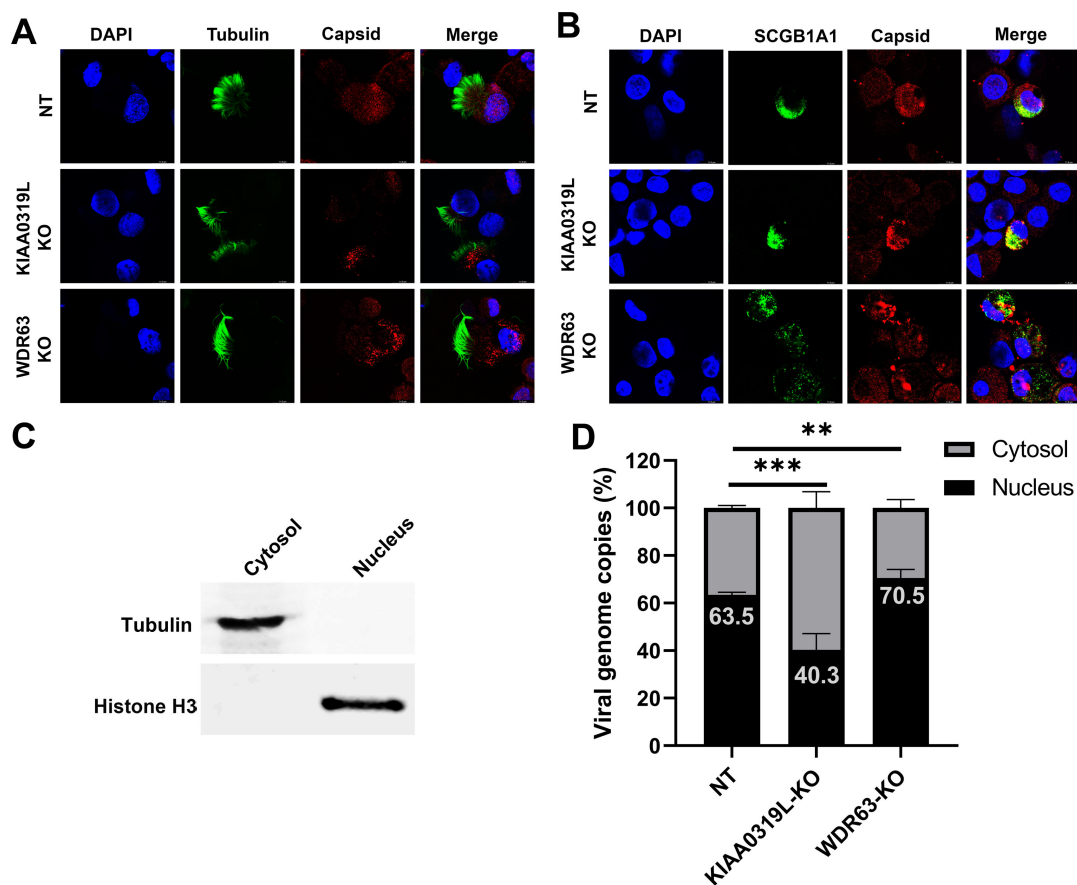
FIG 9 Localization of the AAV2.5T capsid in transduced HAE-ALI cultures. AAV2.5T was used to apically transduce HAE-ALI cultures as indicated at an MOI of 20,000. (A and B) rAAV2.5T capsid staining. At 3 days post-transduction, cells were digested off the transwell membranes and cytospun onto slides. The slides were fixed and permeabilized, followed by co-immunostaining of the ciliated cell marker (tubulin, panel A) or club cell marker (SCGB1A1, panel B) with the AAV2.5T capsid. The stained cells were subjected to imaging under confocal microscopy at a magnification of ×100 (CSU-W1 SoRa, Nikon). (C and D) rAAV2.5T genome distribution. At 3 days post-transduction, cells in the transwell were washed with Accutase three times and then dissociated by incubation with Accutase for 1 hour. After washing, a cell fraction extraction kit (Thermo Fisher) was used to extract the cytosol and nucleus. (C) Western blotting of the cytosol and nucleus fractions extracted from the non-target control HAE-ALI cultures using anti-tubulin and anti-histone H3, respectively. (D) Quantification of the viral genome in each fraction. Viral DNA was extracted from each fraction and quantitated using qPCR. Error bars represent the standard error of the mean (SEM) from three transwell replicates.

prevent the nuclear import of the vector. Notably, immunofluorescence assays found a significant absence of the vector particles within the nuclei of the cells in transduced HAE-ALI$^{\Delta KIAA0319L}$, but substantial viral genomes (40.3%) were still detectable in the nuclear fraction extracted from the transduced HAE-ALI$^{\Delta KIAA0319L}$. We reason this to the limitation of the fractionation method, as the results align with similar experiments carried out in a previously published study (26).

Taken together, our results suggest that KIAA0319L and WDR63 are essential host factors for rAAV2.5T transduction in HAE-ALI cultures. KIAA0319L-KO did not impact the internalization of the rAAV2.5T vector but decreased the nuclear import of the vector in HAE-ALI. Thus, the critical role of KIAA0319L is confined to the intracellular trafficking of the vector to the nucleus. In contrast, WDR63-KO significantly increased the nuclear import of rAAV2.5T, suggesting that WDR63 may prevent the nuclear import of the vector.

DISCUSSION

rAAVs enter cells and exhibit tissue tropism through a multistep process involving viral attachment, internalization, trafficking, and productive transduction (nuclear import, uncoating, and transgene expression). The exact mechanisms can vary depending on the AAV serotype and the target cell type. While the tropism is considered broad in general, rAAVs inefficiently transduce lung airways from the apical side. rAAV2.5T is an AAV variant developed from directed evolution for the treatment of CF lung disease via gene therapy. It has demonstrated a higher efficiency in correcting the deficient Cl^- transportation in the HAE-ALI cultures derived from the lung donors of CF patients following apical transduction when compared to rAAV1 (27), which is the most efficient airway transduction vector from naturally occurring AAV serotypes (28). rAAV1 uses both α2,3 and α2,6 sialic acid residues that are present on N-linked glycoproteins as primary attachment receptors for transduction (29), but rAAV2.5T utilizes only α2,3 N-linked sialic acid residues, like AAV5 (18). While a previous study found the lack of endogenous KIAA0319L expression on the apical surface membrane of HAE-ALI, suggesting that efficient rAAV2.5T transduction is accomplished with a KIAA0319L-independent pathway (20), nothing is known about the mechanism underlying the highly efficient gene delivery of rAAV2.5T into human airway epithelia. In this study, we identified that KIAA0319L is a critical factor for rAAV2.5T transduction of airway epithelia but not for vector internalization by acting as the proteinaceous cellular receptor. In addition, we confirmed that WDR63, a less studied WD repeat domain-containing protein, is an essential host factor for rAAV2.5T transduction in human airway epithelia. Similar to KIAA0319L, WDR63 does not contribute to vector internalization. Importantly, we also identified that novel host factors, PDE4A and GPR174, play a moderate role in rAAV2.5T transduction in HeLa cells.

AAVs bind to proteoglycans as a primary attachment receptor, which facilitates cellular uptake/internalization (30); for example, AAV2 binds to heparan sulfate proteoglycans (HSPGs) (31, 32). Post attachment, AAVs are thought to employ a proteinaceous receptor(s) to mediate cellular entry. The identification of proteinaceous receptors for AAV uptake has been a focus of AAV research for a long time (33, 34). A 150-kDa AAV-binding protein was initially revealed by Mizukami et al. in 1996 on a virus overlay assay (35). In 2016, Carette and Chapman's labs collaboratively identified KIAA0319L as a multi-serotype AAV receptor (AAVR) and demonstrated the physical interaction between KIAA0319L and AAV2 (12). KIAA0319L is both an N- and O-glycosylated protein with a size of 150 kDa (14), and the glycosylation of KIAA0319L is not essential for AAV2-AAVR interactions or AAV2 transduction. KIAA0319L is significantly involved in the transduction of AAV1-3 and AAV5-9; however, it is not essential for AAV4 transduction (13).

The capsid of AAV2.5T only has one mutation of A581T that differed from AAV5 in the major capsid protein VP3; however, rAAV2.5T transduction exhibits a tropism to human airway epithelia much higher than that of its parent AAV5 (15). Molecular modeling of AAV2.5T showed that the A581T mutation occurs at the mouth of the predicted AAV5 sialic acid binding pocket. An anti-KIAA0319L antibody blocked the transduction of AAV2 from the basolateral side but not AAV2.5T from the apical side, suggesting that there is an unknown unique apical receptor for AAV2.5T (20). Since the anti-KIAA0319L polyclonal antibody was used at a single dose (50 µg/mL), it remains possible that KIAA0319L plays a role in the apical transduction of HAE. In this study, we used an sgRNA library and performed two rounds of screening in HeLa S3 cells to identify AAV2.5T receptors and host essential factors, as monolayer airway epithelial cells, e.g., CuFi-8, are less transducible. Our screening results showed that KIAA0319L is the top-ranking gene restricting rAAV2.5T transduction in HeLa cells. When knocked out in human airway epithelia, a nearly 95% reduction in rAAV2.5T transduction was observed from both apical and basolateral infections. However, in our study, the knockout of KIAA0319L did not significantly decrease vector internalization, regardless of whether a high or low MOI was used (data not shown). Interestingly, rAAV2.5T internalization
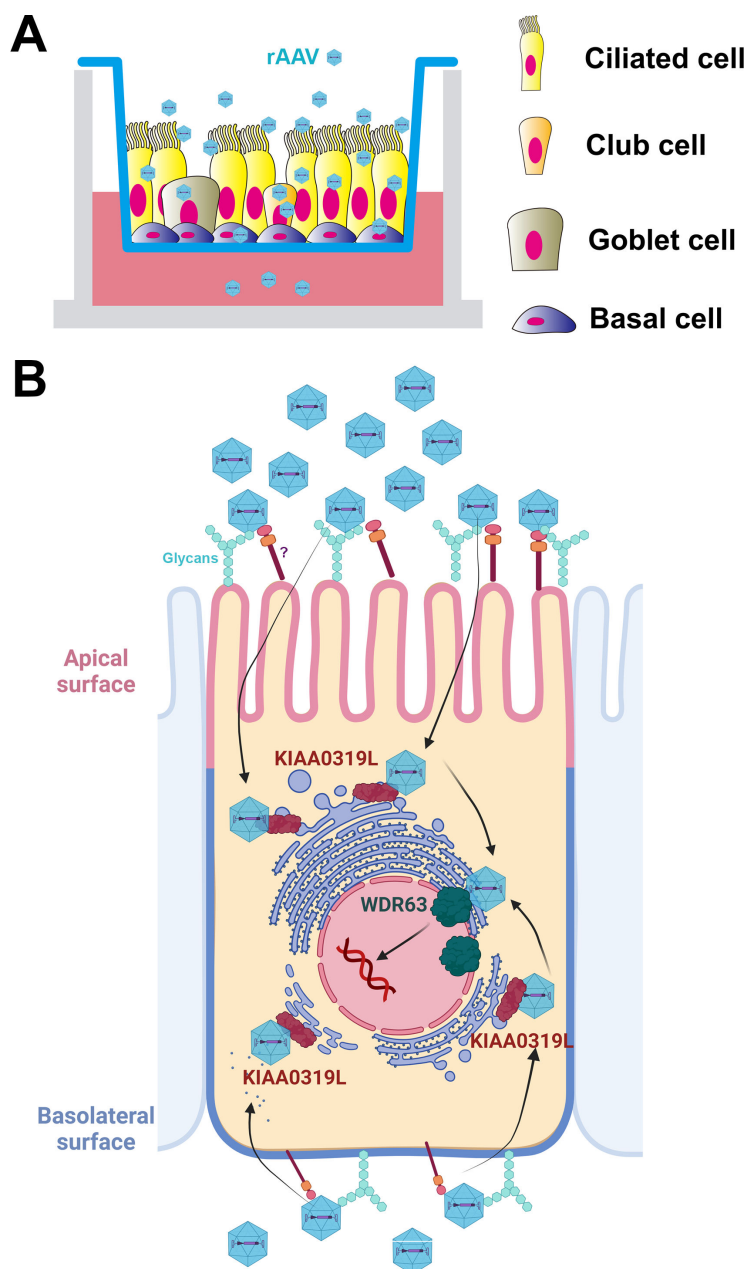
FIG 10 A model of rAAV2.5 transduction of HAE-ALI. (A) Well-differentiated HAE-ALI model. Human airway epithelial cells are differentiated on Transwell inserts at an air-liquid interface (ALI) for 3–4 weeks. Four major types of epithelial cells in the well-differentiated polarized HAE-ALI cultures, basal, ciliated, goblet, and club cells, are diagrammed in the Transwell insert. rAAV2.5T transduces the four major types of airway epithelial cells. (B) AAV2.5T entry of HAE. Represented is a ciliated cell diagram with the nucleus surrounded by the trans-Golgi network (TGN) and endoplasmic reticulum (ER). AAV2.5T binds glycans on and enters into airway epithelial cells of the HAE-ALI cultures from either the apical or basolateral side through an unknown proteinaceous receptor (marked with "?") independent of KIAA0319L. The capsid likely interacts with KIAA0319L during entry and localizes to the TGN, followed by nuclear input. WDR63 likely plays a role in transgene expression in the nucleus, and its role in rAAV transduction is likely both serotype- and cell type-independent. Created with BioRender.

decreased by ~50% after knocking out KIAA0319L in HeLa cells compared to WT HeLa cells, suggesting that the function of KIAA0319L might differ based on the cell type. We propose that KIAA0319L plays an important role in the intracellular trafficking of rAAV2.5T in airway epithelia (Fig. 10). After internalization, AAV2.5T interacts with KIAA0319L in the endocytosed vesicle, which then facilitates vector escape from the TGN or late endosome. This could be the physiological function of KIAA0319L, by binding to an unknown ligand and recycling from the cell surface and endosome to the perinuclear TGN. Thus, our study suggests that there are other cell surface proteins that are required for rAAV2.5T internalization of airway epithelia, which have not been selected in the CRISPR screening in HeLa cells.

We identified novel host factors, WDR63, PDE4A, and GPR174, that play a significant role in rAAV2.5T transduction in HeLa cells, among which WDR63 is confirmed to be essential for rAAV2.5T transduction in human airway epithelia. WDR63 is a WD repeat-containing protein that plays roles as a negative regulator of cell migration, invasion, and metastasis by inhibiting actin polymerization (36). WDR63 has also been shown to be a positive enhancer of osteogenic stem cell differentiation and enhances the expression of *BSP*, *OSX*, and *RUNX2* (37), indicating that WDR63 might be a transcription factor that enhances transgene expression in the nucleus (Fig. 10B). WDR63 is localized in both the nucleus and the cytoplasm and did not colocalize with the vector in cells (Fig. S5). Therefore, it is possible that WDR63 may influence the expression of another host factor that is crucial for rAAV transduction. WDR63 is not required for vector internalization but plays a negative role in AAV2.5T nuclear entry (Fig. 10B). The involvement of WDR63 in rAAV transduction of HAE-ALI was also validated using rAAV2 and rAAV5 (Fig. S6), thereby confirming that the role of WDR63 in rAAV transduction is independent of VP1u and essential for both rAAV2 and rAAV5 transduction. Thus, the role of WDR63 in rAAV transduction is likely both serotype- and cell type-independent. Additional efforts are apparently required to verify the role of PDE4A and GPR174 in rAAV2.5T transduction in human airway epithelia.

HAE cultures derived from primary bronchial epithelial cells isolated from the airways of human lung donors or patients undergoing lung transplantation have been extensively used to study the biology of the respiratory epithelium (38). However, limited by the difficulty of gene knockouts in primary cells with limited proliferative capacity, the HAE-ALI cultures we used were differentiated/polarized from CuFi-8 cells, which are immortalized human airway epithelial cells that were isolated from a cystic fibrosis patient and express hTERT and HPV E6/E7 genes (22). CuFi-8-derived HAE is composed of 50% ciliated cells, 24% basal cells, 22% club cells, and 4% goblet cells, which have a similar composition to the results of single-cell RNA sequencing of nasal epithelial cultures (39). In rAAV2.5T-transduced HAE at an MOI of 20,000 DRPs/cell, about one-third (35.4%) of the airway epithelial cells expressed mCherry, supporting the high transduction efficiency of airway cells. Among all the mCherry-positive (transduced) cells, club cells accounted for 34% and basal cells accounted for ~20%. Both club cells and basal cells are progenitors of the airway epithelium (38, 40). Importantly, basal and club cells can be differentiated into ciliated and goblet cells under certain conditions, such as pathogenic viral infection (41, 42). For cystic fibrosis gene therapy, it is more beneficial to transduce the stem-like cells rather than the ciliated cells (43).

AAV has emerged as a prominent viral vector platform for gene therapy, holding great promise in the treatment of genetic diseases and cancers. However, the underlying biological processes remain largely unexplored. Gaining a comprehensive understanding of the mechanistic basis of rAAV transduction biology will enable us to take advantage of its full potential. The human airway epithelia are composed of multiple cell types, including basal stem cells. AAV transduction of various airway epithelial cells may use different cellular receptors and pathways, which is important for airway gene delivery using AAV vectors. Notably, the requirement of KIAA0319L for highly efficient airway epithelial gene delivery, regardless of basal or apical infection, but not for vector internalization, highlights the unique feature of rAAV2.5T-mediated airway gene delivery.

MATERIALS AND METHODS

Cells and cell culture

Cells

Both HEK293FT (Thermo Fisher) and HeLa cells (ATCC CCL-2) were grown in Dulbecco's Modified Eagle's Medium (DMEM; HyClone #SH30022.01, Cytiva, New York, NY, USA) supplemented with 10% fetal bovine serum (FBS) and 100 units/mL penicillin-streptomycin in a humidified incubator with 5% CO_2 at 37°C. HeLa S3 cells (ATCC CCL-2.2) were grown in Ham F-12 (#10-080-CV; Corning, Corning, NY, USA) supplemented with 10% FBS (#F0926; MilliporeSigma, St. Louis, MO, USA) and 100 units/mL penicillin-streptomycin. Cells were cultured in shaking flasks on an orbital shaker platform at 120 rpm in a humidified incubator with 5% CO_2 at 37°C. The cells were maintained at a low density of 0.1–0.3 million/mL. CuFi-8 cells were immortalized from human primary airway epithelial cells isolated from a cystic fibrosis patient by expressing hTERT and HPV E6/E7 genes (22). They were cultured on collagen-coated 100-mm dishes in PneumaCult-Ex Plus medium (#05040; StemCell, Vancouver, BC, Canada).

Human airway epithelium cultured at an air-liquid interface

Proliferating CuFi-8 cells dissociated from flasks were directly loaded on collagen-coated Transwell permeable supports (#3470; Costar, Corning) with PneumaCult-Ex Plus in both apical and basal chambers. One day after seeding, the media were replaced with PneumaCult-ALI medium (#05001; StemCell) for 1–2 days, and then, the media in the apical chamber were removed. The cells were then differentiated/polarized in Pneuma-Cult-ALI medium at an ALI for 3–4 weeks (44). The maturation of the polarized HAE-ALI cultures derived from CuFi-8 cells was determined by TEER measured with a Millicell ERS-2 volt-ohm meter (MilliporeSigma, Burlington, MA, USA). ALI cultures with a TEER value of >1,000 $\Omega \cdot cm^2$ were used for experiments.

Production of rAAV2.5T vectors

The dual-report rAAV2.5T vector, rAAV2/2.5T.F5tg83luc-CMVmCherry, was produced using a triple-plasmid transfection method using calcium phosphate (28). Briefly, the AAV2 Rep and AAV5 capsid-expressing plasmid pRep2Cap2.5T (15), the adenovirus 5 helper pAd4.1 (45), and the AAV2 transgene plasmid pAV2F5tg83luc-CMVmCherry (46) were transfected at a molar ratio of 1:1:1 into HEK293 cells cultured in 150-mm plate flasks. rAAV2.5T vectors were purified in cesium chloride density gradients, following a method as previously described (28). Vector titers were determined by real-time quantitative polymerase chain reaction (qPCR) using primers and probes specific to the *mCherry* transgene as DNase I-resistant particles per milliliter (46).

Genome-wide CRISPR screening

HeLa S3 cells were transduced with a *Streptococcus pyogenes* (sp)Cas9-expressing lentivirus (#52962; Addgene, Watertown, MA, USA) at an MOI of 20 transduction units (TUs)/cell. At 3 days post-transduction, Blasticidin S, hereafter referred to as "blasticidin" (Thermo Fisher, Waltham, MA, USA), was added at 10 µg/mL to select spCas9-expressing cells. Western blotting and immunofluorescence staining were performed to confirm spCas9 expression. After the cells were expanded to 100 million, human CRISPR Brunello lentiviral pooled libraries (#73179-LV; Addgene) were added to the cell culture at an MOI of 0.25 in the presence of polybrene (Santa Cruz, Dallas, TX, USA). At 24 hours post-transduction, puromycin was added at a concentration of 2 µg/mL to select sgRNA-expressing cells for 1 week to select the blasticidin and puromycin double-resistant (gene edited) cells for proliferation. One hundred million cells were harvested for extraction of gDNA as the unselected control (gDNA^{Ctrl}). Another 100 million cells were transduced with rAAV2.5T at an MOI of 20,000 DRPs/cell, ensuring that over 95% of HeLa S3 cells were transduced. At 3 days post-transduction, the cells were subjected to sorting on a BD

FACSAria III Cell Sorter to select the top 1% mCherry-negative cells at the Flow Cytometry Core Laboratory of the University of Kansas Medical Center. Approximately 1 million mCherry-negative cells were collected and expanded to ~100 million, which underwent the second round of rAAV2.5T transduction and sorting process. Again, ~1 million mCherry-negative cells were collected and expanded to ~100 million cells and were subjected to extraction of gDNA, which was designated as gDNA^{Screen}.

Genomic DNA extraction, NGS, and bioinformatics analysis

gDNA extraction

gDNA samples from the unselected control (gDNA^{Ctrl}) and the second (gDNA^{Screen}) selected group cells were extracted using the Blood and Cell Culture DNA Midi Kit (#13343; QIAGEN, Germantown, MD, USA).

NGS and bioinformatics analysis

The extracted gDNA samples were subjected to PCR-based amplification of guide sequences and indexed according to the protocol from the Broad Institute of MIT and Harvard (47). The PCR amplicons were sequenced with an Illumina NextSeq 2000 platform. All the reads of sgRNAs were analyzed using the MAGeCK software package (48). Significance values were determined after normalization to the control population, and the data were reported as an enrichment score.

The analyzed data were visualized through GraphPad. For visualization purposes, genes were sorted by gene ontology terms. The hits [by $-\log_{10}$(enrichment score)] were then plotted along the *y*-axis and were arbitrarily scattered within their categories along the *x*-axis. The size of the dot was determined according to the selected/unselected fold change.

Western blotting

Cells were dissociated from the flask/transwell and solubilized with RIPA buffer [150 mM NaCl, 1% NP-40, 0.5% sodium deoxycholate, 0.1% sodium dodecyl sulfate (SDS), and 50 mM Tris-HCl, pH 7.4]. The cell lysates were mixed with 5× protein loading buffer and boiled for 10 minutes. Then, the samples were subjected to SDS-10% polyacrylamide gel electrophoresis, followed by transferring the separated proteins onto a nitrocellulose membrane. After blocking with non-fat milk for 1 hour, the membrane was incubated with the primary antibody overnight, followed by incubation with an infrared dye-conjugated IgG (H+L) secondary antibody for 1 hour. Finally, the membrane was imaged on a LI-COR Odyssey imager (LI-COR Biosciences, Lincoln, NB, USA).

rAAV transduction

For HeLa cells, they were seeded overnight in 48-well plates. rAAV2.5T was added to each well at an MOI of 20,000 DRPs/cell. The transduction efficiency was analyzed using a firefly luciferase assay and mCherry intensity at 3 days post-transduction.

For apical transduction of HAE-ALI, 400 µL of PBS-diluted rAAV2.5T was added to the apical chamber of the transwell at an MOI of 20,000 DRPs/cell. Then, 1 mL of culture media with or without 2 µM doxorubicin was added to the basolateral chamber. After 16 hours, all liquid in the apical and basolateral chambers was removed and washed with D-PBS, pH 7.4 (Corning), three times. Fresh culture media were then added to the basolateral chamber.

For basolateral transduction of HAE-ALI, the media in the basolateral chamber were removed and replaced with 1 mL of culture media with or without 2 µM doxorubicin. rAAV2.5T was then directly added to the basolateral chamber at an MOI of 20,000 DRPs/cell. The media in the basolateral chamber were then replaced.

Luciferase assays

Firefly luciferase activity was detected using the Luciferase Assay System (#E4550; Promega, Madison, WI, USA). At 3 days post-transduction for HeLa cells or 5 days post-transduction for HAE-ALI cultures, cell culture media were removed, and cells were lysed in 200 µL per 48-well of Lysis Buffer (Promega), then frozen at −80°C. After thawing, firefly luciferase expression was measured in relative light units on a multi-mode microplate reader (Synergy H1, Agilent).

mCherry quantification

mCherry expression was visualized under an inverted fluorescence microscope (Nikon Ti-S), and the intensity was quantified by ImageJ.

Gene silencing using shRNA-expressing lentiviruses

All of the shRNA-expressing lentiviruses (shRNA-lenti), generated from shRNA cloned pLKO.1-puro, were purchased from MilliporeSigma (Table S2). HeLa cells were seeded in a 24-well plate with 80% cell confluence. After the culture media were removed, shRNA-lenti was added to each well at an MOI of ~10 TUs/cell. The plate was then placed in a humidified incubator with 5% CO_2 at 37°C for 2 hours, followed by the addition of 500 µL of culture media. At 2 days post-transfection, puromycin was added at 2 µg/mL (#P9620; MillporeSigma) to each well to select gene-silenced cells. Western blot assay was performed to confirm the knockdown efficiency.

Generation of gene knockout stable cell lines

pLentiCRISPRv2 constructs

sgRNAs targeting genes, listed in Table S3, were respectively cloned in the plenti-CRISPRv2 vector (49). The lentiCRISPRv2 expressing a scramble sgRNA (5′-GTA TTA CTG ATA TTG GTG GG-3′) was used as an NT control.

gRNA-based lentivirus production

Lentivirus was produced in HEK293FT cells by transient transfection using PEI Max according to a previously published protocol (49). Briefly, individual sgRNA-containing lentiviruses were produced in HEK293FT cells seeded at 4×10^6 cells per 150-mm dish one night before transfection. One hour prior to transfection, the media were changed with fresh media without antibiotics, followed by transfection of psPAX2, pMD2G, and gRNA sequence cloned lentiCRISPR v2 plasmid at a 2:1:2 ratio. PEI Max (#24765; Polysciences Inc.) was added at a mass ratio of 1:3 DNA to PEI Max. The supernatant was collected at 48 hours post-transfection, clarified by centrifugation at 3,000 rpm for 30 minutes, and filtered through a 0.45-µm filter. The filtrated supernatant (lentivirus) was concentrated in a SureSpin 630 rotor in Sovall WX 80 (Thermo Fisher) at 24,000 rpm for 2 hours at 4°C. The concentrated lentiviruses were resuspended in DMEM media and stored at −80°C.

Generation of stable cell lines

HeLa or CuFi-8 cells were seeded at a density of 1×10^5 cells per well in a 24-well plate. For CuFi-8 cells, the plates were collagen-coated. When the cells reached 80% confluence, lentivirus containing sgRNAs was added to each well at ~5 MOI. At 2 days post-transduction, puromycin was added at 2 µg/mL to select for gene knockout cells. The selected cells were then digested and seeded into a 96-well plate at a density of 0.5 cells/well. Once sufficient confluence was reached, the cells in each well were reseeded into a 6-well plate, and Western blot analysis was performed to determine the knockout efficiency.

Vector internalization assay

HAE-ALI cultures were infected with rAAV2.5T at an MOI of 20,000 from the apical or basolateral side. HeLa cells were infected at the same MOI. The cultures/cells were then incubated in a humidified incubator with 5% CO_2 at 37°C for 2 hours before being washed with D-PBS three times. We carried out a vector internalization assay using a previously published method (50). Cells were washed with Accutase (#AT104; Innovative Cell Technologies, Inc.) three times and then incubated with Accutase at 37°C for 1 hour. After washing with PBS three times, viral DNA was collected using Quick-DNA/RNA Pathogen Kits (#R1042; Zymo Research) and quantified by qPCR using mCherry primers/ probes.

Nuclear and cytoplasmic extraction

We fractionated the nucleus vs cytosol fraction of the HAE-ALI cultures using the NE-PER Nuclear and Cytoplasmic Extraction Reagents (#78833; Thermo Fisher).

Immunofluorescence confocal microscopy

For immunofluorescence of intact HAE-ALI cultures, the membrane support of the insert was cut off and fixed in 4% paraformaldehyde in PBS at 4°C overnight. The fixed membrane was washed in D-PBS three times and then split into eight pieces for whole-mount immunostaining. The fixed membrane pieces were permeabilized with 0.5% Triton X-100 in D-PBS for 15 minutes at room temperature and mounted on a slide. The slide was incubated with a primary antibody in D-PBS with 2% FBS for 1 hour at 37°C, followed by washing three times, and was incubated with Alexa 488 and Alexa 594 secondary antibodies, followed by staining of the nuclei with DAPI (4′,6-diamidino-2-phenylindole).

For analysis of the AAV2.5T-transduced cells of HAE-ALI cultures, we dissociated the cells off the supportive membranes of the Transwell inserts by incubation with Accutase. After incubation for 1 hour at 37°C, the cells were completely detached from the membrane and well separated. The cells were then cytocentrifuged onto slides at 1,500 rpm for 3 minutes in a Shandon Cytospin 3 cytocentrifuge. The slides were fixed with 4% paraformaldehyde in D-PBS for 10 minutes and were washed with D-PBS for 5 minutes three times. The fixed cells were permeabilized with 0.5% Triton X-100 for 15 minutes at room temperature. Then, the slide was incubated with one or two primary antibodies (Table S4) in D-PBS with 2% FBS for 1 hour at 37°C. After washing three times, the slide was incubated with Alexa 488- and/or Alexa 594-conjugated secondary antibodies, followed by staining of the nuclei with DAPI.

The slides were visualized under a Leica TCS SP8 or Nikon CSU-W1 SoRa confocal microscope at the Confocal Core Facility of the University of Kansas Medical Center. Images were processed with the Leica Application Suite X software.

Flow cytometry

Sorting of mCherry-positive cells of HAE-ALI

HAE-ALI cultures were pretreated with 2 µM doxorubicin and transduced with AAV2.5T at an MOI of 20,000 DRPs/cell. At 7 days post-transduction, the cells on the insert membrane were treated with Accutase for 1 hour and spun down at $300 \times g$ for 3 minutes. The mCherry-positive cells were sorted using a FACSAria III sorter.

Airway epithelial cell typing

Cells of the HAE-ALI cultures were digested with Accutase for 1 hour. After spinning at $300 \times g$ for 3 minutes, the cells were fixed with 4% PFA and permeabilized with 0.5% Triton X-100 in PBS. The primary antibody for each cell marker was added to the cells at a 1:1,000 dilution and incubated for 1 hour. The cells were then washed with PBS three times, and the corresponding secondary antibody conjugated with Alexa 488 was added

to the cells, followed by incubation for 1 hour. After three washes with PBS, the samples were analyzed by flow cytometry to quantify Alexa 488 fluorescence. Negative control cells were incubated with 3% bovine serum albumin (BSA) and the second antibody.

Statistical analysis

All data were determined with the means and SDs obtained from at least three independent experiments by using GraphPad. Error bars represent means and SDs. Statistical significance (P value) was determined by using an unpaired (Student) t-test for the comparison of the two groups. ****$P < 0.0001$, ***$P < 0.001$, **$P < 0.01$, and *$P < 0.05$ were considered statistically significant, and n.s. represents statistically no significance.

AUTHOR AFFILIATIONS

[1]Department of Microbiology, Molecular Genetics and Immunology, University of Kansas Medical Center, Kansas City, Kansas, USA
[2]Department of Anatomy and Cell Biology, University of Iowa, Iowa City, Iowa, USA
[3]GeneGoCell Inc., San Diego, California, USA

AUTHOR ORCIDs

Siyuan Hao http://orcid.org/0000-0001-5068-9772
Jianming Qiu http://orcid.org/0000-0001-9850-1695

AUTHOR CONTRIBUTIONS

Siyuan Hao, Conceptualization, Data curation, Formal analysis, Investigation, Methodology, Validation, Visualization, Writing – original draft, Writing – review and editing | Xiujuan Zhang, Data curation, Methodology, Writing – review and editing | Kang Ning, Data curation, Investigation, Methodology, Validation, Writing – review and editing | Zehua Feng, Methodology, Resources | Soo Yeun Park, Methodology, Resources | Cagla Aksu Kuz, Methodology, Writing – review and editing | Shane McFarlin, Methodology, Writing – original draft | Donovan Richart, Methodology, Writing – review and editing | Fang Cheng, Methodology, Resources | Elizabeth Yan Zhang, Data curation, Formal

analysis, Software | Aaron Zhang-Chen, Data curation, Formal analysis, Software | Ziying Yan, Conceptualization, Funding acquisition, Project administration, Supervision, Writing – review and editing | Jianming Qiu, Conceptualization, Funding acquisition, Project administration, Supervision, Writing – original draft, Writing – review and editing

DATA AVAILABILITY

All data used to evaluate the conclusions in this study are presented in the paper and/or the supplemental material. NGS data are available from the National Center for Biotechnology Information Sequencing Read Archive (SRA) under accession numbers SRR24507630 and SRR24507271 and BioProject under accession number PRJNA971590.

ADDITIONAL FILES

The following material is available online.

Supplemental Material

Supplemental material (JVI01330-23-s0001.pdf). Fig. S1 to S6 and Tables S2 to S4.
Table S1 (JVI01330-23-s0002.xlsx). Screened gene enrichment score.

REFERENCES

1. Cotmore SF, Agbandje-McKenna M, Canuti M, Chiorini JA, Eis-Hubinger A-M, Hughes J, Mietzsch M, Modha S, Ogliastro M, Pénzes JJ, Pintel DJ, Qiu J, Soderlund-Venermo M, Tattersall P, Tijssen P, ICTV Report Consortium. 2019. ICTV virus taxonomy profile: parvoviridae. J Gen Virol 100:367–368. https://doi.org/10.1099/jgv.0.001212

2. Wang D, Tai PWL, Gao G. 2019. Adeno-associated virus vector as a platform for gene therapy delivery. Nat Rev Drug Discov 18:358–378. https://doi.org/10.1038/s41573-019-0012-9

3. Kuzmin DA, Shutova MV, Johnston NR, Smith OP, Fedorin VV, Kukushkin YS, van der Loo JCM, Johnstone EC. 2021. The clinical landscape for AAV gene therapies. Nat Rev Drug Discov 20:173–174. https://doi.org/10.1038/d41573-021-00017-7

4. Bennett J, Wellman J, Marshall KA, McCague S, Ashtari M, DiStefano-Pappas J, Elci OU, Chung DC, Sun J, Wright JF, Cross DR, Aravand P, Cyckowski LL, Bennicelli JL, Mingozzi F, Auricchio A, Pierce EA, Ruggiero J, Leroy BP, Simonelli F, High KA, Maguire AM. 2016. Safety and durability of effect of contralateral-eye administration of AAV2 gene therapy in patients with childhood-onset blindness caused by RPE65 mutations: a follow-on phase 1 trial. Lancet 388:661–672. https://doi.org/10.1016/S0140-6736(16)30371-3

5. Mueller C, Gernoux G, Gruntman AM, Borel F, Reeves EP, Calcedo R, Rouhani FN, Yachnis A, Humphries M, Campbell-Thompson M, Messina L, Chulay JD, Trapnell B, Wilson JM, McElvaney NG, Flotte TR. 2017. 5 year expression and neutrophil defect repair after gene therapy in alpha-1 antitrypsin deficiency. Mol Ther 25:1387–1394. https://doi.org/10.1016/j.ymthe.2017.03.029

6. Lovric J, Mano M, Zentilin L, Eulalio A, Zacchigna S, Giacca M. 2012. Terminal differentiation of cardiac and skeletal myocytes induces permissivity to AAV transduction by relieving inhibition imposed by DNA damage response proteins. Mol Ther 20:2087–2097. https://doi.org/10.1038/mt.2012.144

7. Mendell JR, Al-Zaidy SA, Rodino-Klapac LR, Goodspeed K, Gray SJ, Kay CN, Boye SL, Boye SE, George LA, Salabarria S, Corti M, Byrne BJ, Tremblay JP. 2021. Current clinical applications of *in vivo* gene therapy with AAVs. Mol Ther 29:464–488. https://doi.org/10.1016/j.ymthe.2020.12.007

8. George LA, Monahan PE, Eyster ME, Sullivan SK, Ragni MV, Croteau SE, Rasko JEJ, Recht M, Samelson-Jones BJ, MacDougall A, Jaworski K, Noble R, Curran M, Kuranda K, Mingozzi F, Chang T, Reape KZ, Anguela XM, High KA. 2021. Multiyear factor VIII expression after AAV gene transfer for hemophilia A. N Engl J Med 385:1961–1973. https://doi.org/10.1056/NEJMoa2104205

9. Riyad JM, Weber T. 2021. Intracellular trafficking of adeno-associated virus (AAV) vectors: challenges and future directions. Gene Ther 28:683–696. https://doi.org/10.1038/s41434-021-00252-y

10. Samulski RJ, Muzyczka N. 2014. AAV-mediated gene therapy for research and therapeutic purposes. Annu Rev Virol 1:427–451. https://doi.org/10.1146/annurev-virology-031413-085355

11. Meyer NL, Chapman MS. 2022. Adeno-associated virus (AAV) cell entry: structural insights. Trends Microbiol 30:432–451. https://doi.org/10.1016/j.tim.2021.09.005

12. Pillay S., Meyer NL, Puschnik AS, Davulcu O, Diep J, Ishikawa Y, Jae LT, Wosen JE, Nagamine CM, Chapman MS, Carette JE. 2016. An essential receptor for adeno-associated virus infection. Nature 539:108–112. https://doi.org/10.1038/nature19835

13. Dudek AM, Pillay S, Puschnik AS, Nagamine CM, Cheng F, Qiu J, Carette JE, Vandenberghe LH. 2018. An alternate route for adeno-associated virus (AAV) entry independent of AAV receptor. J Virol 92:e02213-17. https://doi.org/10.1128/JVI.02213-17

14. Pillay S, Zou W, Cheng F, Puschnik AS, Meyer NL, Ganaie SS, Deng X, Wosen JE, Davulcu O, Yan Z, Engelhardt JF, Brown KE, Chapman MS, Qiu J, Carette JE, Banks L. 2017. AAV serotypes have distinctive interactions with domains of the cellular receptor AAVR. J Virol 91:e00391-17. https://doi.org/10.1128/JVI.00391-17

15. Excoffon K, Koerber JT, Dickey DD, Murtha M, Keshavjee S, Kaspar BK, Zabner J, Schaffer DV. 2009. Directed evolution of adeno-associated virus to an infectious respiratory virus. Proc Natl Acad Sci U S A 106:3865–3870. https://doi.org/10.1073/pnas.0813365106

16. Ostedgaard LS, Rokhlina T, Karp PH, Lashmit P, Afione S, Schmidt M, Zabner J, Stinski MF, Chiorini JA, Welsh MJ. 2005. A shortened adeno-associated virus expression cassette for CFTR gene transfer to cystic fibrosis airway epithelia. Proc Natl Acad Sci U S A 102:2952–2957. https://doi.org/10.1073/pnas.0409845102

17. Tang Y, Fakhari S, Huntemann ED, Feng Z, Wu P, Feng WY, Lei J, Yuan F, Excoffon KJ, Wang K, Limberis MP, Kolbeck R, Yan Z, Engelhardt JF. 2023. Immunosuppression reduces rAAV2.5T neutralizing antibodies that limit efficacy following repeat dosing to ferret lungs. Mol Ther Methods Clin Dev 29:70–80. https://doi.org/10.1016/j.omtm.2023.02.015

18. Dickey DD, Excoffon KJDA, Koerber JT, Bergen J, Steines B, Klesney-Tait J, Schaffer DV, Zabner J. 2011. Enhanced sialic acid-dependent endocytosis explains the increased efficiency of infection of airway epithelia by a novel adeno-associated virus. J Virol 85:9023–9030. https://doi.org/10.1128/JVI.05154-11

19. Afione S, DiMattia MA, Halder S, Di Pasquale G, Agbandje-McKenna M, Chiorini JA. 2015. Identification and mutagenesis of the adeno-associated virus 5 sialic acid binding region. J Virol 89:1660–1672. https://doi.org/10.1128/JVI.02503-14

20. Hamilton BA, Li X, Pezzulo AA, Abou Alaiwa MH, Zabner J. 2019. Polarized AAVR expression determines infectivity by AAV gene therapy vectors. Gene Ther 26:240–249. https://doi.org/10.1038/s41434-019-0078-3

21. Meisen WH, Nejad ZB, Hardy M, Zhao H, Oliverio O, Wang S, Hale C, Ollmann MM, Collins PJ. 2020. Pooled screens identify GPR108 and TM9SF2 as host cell factors critical for AAV transduction. Mole Therapy - Meth & Clinical Dev 17:601–611. https://doi.org/10.1016/j.omtm.2020.03.012

22. Zabner J, Karp P, Seiler M, Phillips SL, Mitchell CJ, Saavedra M, Welsh M, Klingelhutz AJ. 2003. Development of cystic fibrosis and noncystic fibrosis airway cell lines. Am J Physiol Lung Cell Mol Physiol 284:L844–54. https://doi.org/10.1152/ajplung.00355.2002

23. Yan Z, Zak R, Zhang Y, Ding W, Godwin S, Munson K, Peluso R, Engelhardt JF. 2004. Distinct classes of proteasome-modulating agents cooperatively augment recombinant adeno-associated virus type 2 and type 5-mediated transduction from the apical surfaces of human airway epithelia. J Virol 78:2863–2874. https://doi.org/10.1128/jvi.78.6.2863-2874.2004

24. Davis JD, Wypych TP. 2021. Cellular and functional heterogeneity of the airway epithelium. Mucosal Immunol 14:978–990. https://doi.org/10.1038/s41385-020-00370-7

25. Pillay S, Carette JE. 2017. Host determinants of adeno-associated viral vector entry. Curr Opin Virol 24:124–131. https://doi.org/10.1016/j.coviro.2017.06.003

26. Dudek AM, Zabaleta N, Zinn E, Pillay S, Zengel J, Porter C, Franceschini JS, Estelien R, Carette JE, Zhou GL, Vandenberghe LH. 2020. GPR108 is a highly conserved AAV entry factor. Mol Ther 28:367–381. https://doi.org/10.1016/j.ymthe.2019.11.005

27. Tang Y, Yan Z, Lin S, Huntemann ED, Feng Z, Park S-Y, Sun X, Yuen E, Engelhardt JF. 2020. Repeat dosing of AAV2.5T to ferret lungs elicits an antibody response that diminishes transduction in an age-dependent manner. Mol Ther Methods Clin Dev 19:186–200. https://doi.org/10.1016/j.omtm.2020.09.008

28. Yan Z, Lei-Butters DCM, Keiser NW, Engelhardt JF. 2013. Distinct transduction difference between adeno-associated virus type 1 and type 6 vectors in human polarized airway epithelia. Gene Ther 20:328–337. https://doi.org/10.1038/gt.2012.46

29. Wu Z, Miller E, Agbandje-McKenna M, Samulski RJ. 2006. Alpha2,3 and alpha2,6 N-linked sialic acids facilitate efficient binding and transduction by adeno-associated virus types 1 and 6. J Virol 80:9093–9103. https://doi.org/10.1128/JVI.00895-06

30. Madigan VJ, Asokan A. 2016. Engineering AAV receptor footprints for gene therapy. Curr Opin Virol 18:89–96. https://doi.org/10.1016/j.coviro.2016.05.001

31. Summerford C, Samulski RJ. 1998. Membrane-associated heparan sulfate proteoglycan is a receptor for adeno-associated virus type 2 virions. J Virol 72:1438–1445. https://doi.org/10.1128/JVI.72.2.1438-1445.1998

32. Qiu J, Handa A, Kirby M, Brown KE. 2000. The interaction of heparin sulfate and adeno-associated virus 2. Virology 269:137–147. https://doi.org/10.1006/viro.2000.0205

33. Qiu J, Mizukami H, Brown KE. 1999. Adeno-associated virus 2 co-receptors. Nat Med 5:467–468. https://doi.org/10.1038/8328

34. Qiu J, Brown KE. 1999. Integrin alphaVbeta5 is not involved in adeno-associated virus type 2 (AAV2) infection. Virology 264:436–440. https://doi.org/10.1006/viro.1999.0010

35. Mizukami H, Young NS, Brown KE. 1996. Adeno-associated virus type 2 binds to a 150-kilodalton cell membrane glycoprotein. Virology 217:124–130. https://doi.org/10.1006/viro.1996.0099

36. Zhao K, Wang D, Zhao X, Wang C, Gao Y, Liu K, Wang F, Wu X, Wang X, Sun L, Zang J, Mei Y. 2020. WDR63 inhibits Arp2/3-dependent actin polymerization and mediates the function of p53 in suppressing metastasis. EMBO Rep 21:e49269. https://doi.org/10.15252/embr.201949269

37. Diao S, Yang DM, Dong R, Wang LP, Wang JS, Du J, Wang SL, Fan Z. 2015. Enriched trimethylation of lysine 4 of histone H3 of WDR63 enhanced osteogenic differentiation potentials of stem cells from apical papilla. J Endod 41:205–211. https://doi.org/10.1016/j.joen.2014.09.027

38. Fulcher ML, Gabriel S, Burns KA, Yankaskas JR, Randell SH. 2005. Well-differentiated human airway epithelial cell cultures. Methods Mol Med 107:183–206.

39. Ruiz García S, Deprez M, Lebrigand K, Cavard A, Paquet A, Arguel M-J, Magnone V, Truchi M, Caballero I, Leroy S, Marquette C-H, Marcet B, Barbry P, Zaragosi L-E. 2019. Novel dynamics of human mucociliary differentiation revealed by single-cell RNA sequencing of nasal epithelial cultures. Development 146:dev177428. https://doi.org/10.1242/dev.177428

40. Konkimalla A, Konishi S, Kobayashi Y, Kadur Lakshminarasimha Murthy P, Macadlo L, Mukherjee A, Elmore Z, Kim S-J, Pendergast AM, Lee PJ, Asokan A, Knudsen L, Bravo-Cordero JJ, Tata A, Tata PR. 2022. Multi-apical polarity of alveolar stem cells and their dynamics during lung development and regeneration. iScience 25:105114. https://doi.org/10.1016/j.isci.2022.105114

41. Hao S, Ning K, Kuz CA, Vorhies K, Yan Z, Qiu J. 2020. Long-term modeling of SARS-CoV-2 infection of in vitro cultured polarized human airway epithelium. mBio 11:e02852-20. https://doi.org/10.1128/mBio.02852-20

42. El-Badrawy MK, Shalabi NM, Mohamed MA, Ragab A, Abdelwahab HW. 2016. Stem cells and lung regeneration. IJSC 9:31–35. https://doi.org/10.15283/ijsc.2016.9.1.31

43. Yan Z, McCray PB, Engelhardt JF. 2019. Advances in gene therapy for cystic fibrosis lung disease. Hum Mol Genet 28:R88–R94. https://doi.org/10.1093/hmg/ddz139

44. Yan Z, Deng X, Qiu J. 2020. Human bocavirus 1 infection of well-differentiated human airway epithelium. Curr Protoc Microbiol 58:e107. https://doi.org/10.1002/cpmc.107

45. Yan Z., Keiser NW, Song Y, Deng X, Cheng F, Qiu J, Engelhardt JF. 2013. A novel chimeric adenoassociated virus 2/human bocavirus 1 parvovirus vector efficiently transduces human airway epithelium. Mol Ther 21:2181–2194. https://doi.org/10.1038/mt.2013.92

46. Wang Z, Cheng F, Engelhardt JF, Yan Z, Qiu J. 2018. Development of a novel recombinant adeno-associated virus production system using human bocavirus 1 helper genes. Mol Ther Methods Clin Dev 11:40–51. https://doi.org/10.1016/j.omtm.2018.09.005

47. Sanson KR, Hanna RE, Hegde M, Donovan KF, Strand C, Sullender ME, Vaimberg EW, Goodale A, Root DE, Piccioni F, Doench JG. 2018. Optimized libraries for CRISPR-Cas9 genetic screens with multiple modalities. Nat Commun 9:5416–07901. https://doi.org/10.1038/s41467-018-07901-8

48. Li W, Xu H, Xiao T, Cong L, Love MI, Zhang F, Irizarry RA, Liu JS, Brown M, Liu XS. 2014. MAGeCK enables robust identification of essential genes from genome-scale CRISPR/Cas9 knockout screens. Genome Biol 15:554. https://doi.org/10.1186/s13059-014-0554-4

49. Ning K, Kuz CA, Cheng F, Feng Z, Yan Z, Qiu J. 2023. Adeno-associated virus monoinfection induces a DNA damage response and DNA repair that contributes to viral DNA replication. mBio 14:e0352822. https://doi.org/10.1128/mbio.03528-22

50. Ning K, Zou W, Xu P, Cheng F, Zhang EY, Zhang-Chen A, Kleiboeker S, Qiu J. 2023. Identification of AXL as a co-receptor for human parvovirus B19 infection of human erythroid progenitors. Sci Adv 9:eade0869. https://doi.org/10.1126/sciadv.ade0869